The effect of warm falls on the development of an insect pest: Diapause in the eastern spruce budworm (*Choristoneura fumiferana*)

By

Jona Lopez Pedersen

A thesis submitted to the Department of Biology and the Faculty of Gradate Studies Committee, in partial fulfillment of the requirements for the degree of Master of Science

St. Francis Xavier University

Antigonish, Nova Scotia

Abstract

The eastern spruce budworm (Lepidoptera: Tortricidae: *Choristoneura fumiferana*) overwinters as a second-instar larva. In early fall, larvae enter a dormant state known as diapause and remains dormant during winter. Yet we know little about the physiological processes governing their diapause development. Recent studies (Roe et al., 2024) suggest that temperature in early diapause affects the spruce budworm's ability to complete diapause during winter. In this thesis, I tested the hypothesis that exposure to warmer temperatures in fall accelerates early diapause development. I predicted that developmental traits in early diapause would be differentially expressed between budworm exposed to cool or warm temperatures. To investigate the effects of temperature on early diapause, I exposed larvae to cool (10 °C) or warm (20 °C) temperatures for up to 10 weeks of fall conditions. Larvae were sampled at eight time points during these 10 weeks to measure gene expression (via transcriptomics) and survival (motility). Additionally, I performed a separate 17-day fall and 18-week winter simulation, to whether the hibernaculum—a silken, cocoon-like structure—affected budworm overwintering survival. Larval motility decreased over time, especially at warm temperatures or in the absence of the hibernaculum. Finally, I identified potential candidates for temperature-dependent gene expression during budworm diapause.

Acknowledgements

This research was conducted at St. FX University, located within the unceded and traditional territory of the Mi'kmaw people.

A special thank you to my advisor, Dr. Jantina Toxopeus, a beyond amazing mentor and scientist. I will always treasure my time in the Stress FX lab and everything I've learned here.

Thank you to my advisory committee, Dr. Tammy Rodela and Dr. Katie Marshall, for their excellent guidance and insights on this project. Additional thanks to Dr. Jackie Lebenzon for being my external examiner.

Thank you to the budworm wranglers at the Great Lake Forestry Centre: Dr. Amanda Roe, Ashlyn Wardlaw, and Alice Liu, as well as the wranglers beyond: Dr. Katie Marshall, Laura-Anne Browning, Maranda van Oirschot, Teresa Keenan, and Kenechukwu Ojukwu. I would also like to thank the Stress FX lab for their support, and the McNichol and Rodela labs for sharing materials for the dispersal experiment with me.

Thank you to Dr. Alex Torson, Dr. Karin van der Burg, and Dr. Alice Dennis, who answered questions about code for my data analysis.

And thank you to Natural Resources Canada and the Nova Scotia Graduate Scholarship for funding this project.

Dedication

Til mamma, som lærte meg forundring og respekt for naturen.

To Erin, whose support means the world.

And *Cf*10-F_{33}, the budworm behind it all.

Table of Contents

List of Tables

List of Figures

List of Abbreviations

°C	Degree centigrade
ca	Circa
*Cf*AFP	*Choristoneura fumiferana* antifreeze protein
*Cf*DAP	*Choristoneura fumiferana* diapause-associated protein
*Cf*HSP	*Choristoneura fumiferana* heat shock protein
G3P	Glyceraldehyde 3-phosphate
GLFC	Great Lakes Forestry Centre
GO	Gene Ontology
HSP	Heat shock protein
IGFBP	Insulin-like growth factor binding protein
IPQL	Insect Production and Quarantine Laboratories
JH	Juvenile hormone
L1	First-instar larvae
L2	Second-instar larvae
mRNA	messenger RNA
rRNA	ribosomal RNA
mSP	maSigPro
PCA	Principal component analysis
PC1	Principal component 1
PC2	Principal component 2
PTTH	Prothoracicotropic hormone
s	Seconds
S:A	Significant:Annotated
TOR	Target of rapamycin

Chapter 1: Introduction

During times of seasonal adversity, like harsh winters or warm summers, many insect species enter a state of dormancy known as diapause (Denlinger, 2022). Diapausing insects exhibit similar characteristics such as arrested cell cycle development, increased stress tolerance, and suppression of physiological processes like metabolism (Košťál, 2006). While diapause shares similarities with other dormancies in mammals, birds, reptiles, and amphibians (Wilsterman et al., 2021), insects also face unique physiological and environmental challenges. Their ectothermic nature limits their heat source to ambient or external temperatures (Sinclair et al., 2013), which can be especially stressful for overwintering insects that must survive in cold environments. As future winters are projected to be more varied and extreme, insects will likely need to contend with changing climates (Marshall et al., 2020). Seasonal changes may affect the environmental cues that dictate dormancy periods and life cycle events, as well as insects' relationships to the plants they may have co-evolved with. This thesis examines the relationship between diapause and warm fall temperatures in an insect pest of spruce-fir forests, the eastern spruce budworm (*Choristoneura fumiferana*). These findings may inform how changing climates will alter the development and overwintering behaviour of a diapausing forest pest, with implications for spring emergence and population ranges.

Diapause: An Insect Dormancy

Diapause & Post-Diapause Development

Diapause is a developmental process which progresses through several distinct phases that, like morphogenesis, are not static, and may vary between species, life stages, or populations (Košťál, 2006; Denlinger, 2022). During morphogenesis, the insect progresses through typical life stages, developing from an egg and eventually to an adult. In the face of seasonal adversity, many insects reroute their developmental program from a state of morphogenesis to a state of diapause (Košťál, 2006). Diapause is stage-specific to a given insect's life cycle, occurring at the embryonic, nymph, larval, pupal, or adult stage (Denlinger, 2022). Some species even diapause more than once, such as the cabbage butterfly, *Pieris melete*, which enters a pupal diapause both in summer and winter (Xue et al., 1997). While diapause arose multiple times across the world and throughout the evolutionary history of insects (Denlinger, 2022), different insect groups share many of the same discrete diapause characteristics, especially within life stages (Wilsterman et al., 2021; Ragland & Keep, 2017). Environmental signals like daylength and temperature vary longitudinally and temporally, affecting diapause timing in different species and populations over time. Although diapause in temperate species is more prevalent in the literature, this is likely attributed to how understudied diapause is in tropical species (Denlinger, 2022).

Both environmental and genetic factors may affect whether insects enter diapause, resulting in differences in diapause entry between species, populations, and individuals. In obligate entry, diapause may be induced without any external cues. Rather, it is a genetically programmed event occurring at a specific time in an insect's life stage (Košťál, 2006). On the other hand, facultative entry into diapause relies on cues such as temperature or photoperiod (i.e., daylength), and is a plastic or unfixed response to environmental signals. The cherry fruit fly, *Rhagoletis cerasi*, enters an obligate pupal diapause to overwinter, whereas only a proportion of the population enters a second facultative diapause (Moraiti & Papadopoulos, 2017). This successive diapause is cued by insufficient cold exposure during winter, allowing a proportion of the population to delay spring emergence for another year, potentially increasing synchronicity with its host plant. Plasticity in diapause entry may occur between populations rather than within, as exemplified by the green-veined white butterfly, *Pieres napi* (Steward et al., 2024). In Sweden, populations of *P. napi* experience variable voltinism, the number of generations in a year, depending on longitudinal location. Arctic populations are univoltine and diapause every generation in preparation of winter, whereas southern populations are multivoltine and diapause every other generation. Both populations have a facultative diapause entry, but the Arctic population functionally undergoes obligate diapause. This plasticity suggests that variable environmental conditions pre-winter, such as the colder temperatures or extensive darkness of Arctic photoperiods, facilitate different diapause responses.

During diapause, the insect's developmental program progresses through several distinct phases, referred to as initiation, maintenance, and termination (Košťál, 2006). Whether diapause entry is obligate or facultative, once the insect is committed to the diapause program, it will begin initiation, a shift from allocating available energy towards growth or reproduction to conserving energy for basal maintenance and physiological stress adjustments. For example, 7-10 days after pupation, apple maggot flies (*Rhagoletis pomonella*) depress their metabolic rate to about 8% of that of their non-diapausing counterparts (Ragland et al., 2009). A maintenance period follows initiation, at which point the insect will remain in diapause even if environmental conditions become optimal for morphogenesis and energy production. In Greece, the ladybeetle *Hippodamia* *undecimnotata* retreats to the mountains where they undergo an adult diapause between July and August (Katsoyannos et al., 2005). If transferred from their diapause sites to rearing conditions in a lab, the beetles fail to reproduce for 2-3 months, indicating that diapause maintenance delays oviposition even if conditions become permissible for egg-laying. Diapause then concludes in the termination phase, either as a direct result of maintenance coming to an end or an interplay of environmental and hormonal signals (Košťál, 2006; Hahn & Denlinger, 2011). The fly *Chymomyza costata* enters a larval diapause which can be terminated by either long-term cold exposure or longer photoperiods (Košťál et al., 2000; Košťál et al., 2017). Similarly, *R. cerasi* terminates diapause after meeting a population-dependent chilling requirement, aligning with that of its dormant host plant (Moraiti & Papadopoulos, 2017).

Although termination concludes diapause development, some insects remain dormant in a state referred to as post-diapause quiescence (Košťál, 2006). Quiescence is characterized as an inhibition of development caused directly by environmental conditions that are not permissive for growth and development, whereas diapause unfolds in anticipation of seasonal challenges. Following the summer diapause of the aforementioned *H. undecimnotata*, the ladybeetle transitions to a quiescent state from September to January (Katsoyannos et al., 2005). While transfer from dormancy sites to rearing conditions during diapause maintenance delayed oviposition by months, transfer during quiescence only delayed reproduction by 2-4 weeks. In other words, quiescent insects return to morphogenesis under permissive conditions more readily than diapausing insects. A quiescent period after diapause termination allows insects to respond flexibly to variable seasons, facilitating a synchronous seasonal emergence and for individuals to reproduce at similar times (Denlinger, 2022).

Temperature-Dependent Diapause Development

An ectotherm's "performance" can be plotted as a function of temperature using a thermal performance curve (Huey & Stevenson, 1979), and recent models have used this framework to understand diapause developmental rates (Toxopeus et al., 2024; von Schmalensee et al., 2024). Although chilling seems to be required for the diapause process, diapausing *R. pomonella* pupae require more time to complete diapause when exposed to chilling conditions (15 °C or below) for longer durations (Toxopeus et al., 2024). Furthermore, diapause development progressed more quickly for flies diapausing at 21 °C instead of ≤ 15 °C, measured in terms of pupal eclosion. A similar temperature-dependency has been observed in *P. napi*, which also undergoes a pupal diapause (von Schmalensee et al., 2024). When exposed to winter temperatures (between –6 and 15 °C) followed by 20 °C post-winter temperatures, *P. napi* pupae terminate diapause most frequently if exposed to 1–2 °C. Conversely, *P. napi* terminates diapause at a lower rate if exposed to temperatures below or above 1–2 °C, indicating slower diapause progression. These studies demonstrate possible temperature-dependency in the diapause of both lepidopteran and dipteran species (Toxopeus et al., 2024; von Schmalensee et al., 2024). While temperature-dependency seemingly occurs in the pupal diapause of these species, researchers have yet to identify this process in other insect life stages.

In a temperature-dependent diapause model, diapause development occurs within a specific temperature range, progressing at a rate responding to specific temperatures

(Toxopeus et al., 2024; von Schmalensee et al., 2024; Fig. 1.1A.). No diapause development occurs outside of the range of permissive temperatures. At lower temperatures, diapause development progresses slower, increasing as temperatures rise until reaching a maximum, at which point the developmental rate decreases again (Fig. 1.1A.). Although Fig. 1.1A portrays the typical shape of a thermal performance curve, shapes may vary, as in Fig. 1.1B. When thermal performance curves are applied to diapause termination and post-diapause developmental rates in *P. napi*, diapause termination demonstrates a right-skewed termination rate (Fig. 1.1B) while post-diapause development (morphogenesis) demonstrates a more typical shape, similar to Fig. 1.1A (von Schmalensee et al., 2024). If the thermal performance curves for diapause termination and post-diapause development overlap, as observed by von Schmalensee et al. (2024), individuals at temperatures below the overlap may remain in post-diapause quiescence, while those at temperatures within the overlap may proceed to post-diapause development.

Using a thermal performance curve to model diapause developmental rates presents some limitations, considering the trade-offs between thermal sensitivity and energy drain (Sinclair et al., 2012). Diapause progression at high temperatures may be strictly hypothetical, as warm temperatures increase metabolism and conflict with the insect's energy budget and survival (Hahn & Denlinger, 2011). As populations in cooler environments are less susceptible to energy drain compared to populations in warmer environments, the thermal sensitivity at which diapause development occurs may be broader for the population in the cooler environment (Sinclair et al., 2012; Clarke, 1993). If a population in a warmer environment (e.g., a lower elevation or latitude) had a similarly broad thermal sensitivity, diapause development and metabolic rate would be more likely to conflict, decreasing successful completion of diapause. Different developmental stages of diapause, like initiation, maintenance, and termination, may also differ in thermal sensitivity (Toxopeus et al., 2024; Košťál, 2006). For instance, chilled *R. pomonella* in early diapause are more sensitive to low temperatures while pupae in late diapause are more sensitive to higher temperatures (Toxopeus et al., 2024). As such, the thermal performance curve portrayed in Fig. 1.1A. will be broader or narrower depending on variables specific to timing, environments, populations, and individuals (Toxopeus et al., 2024; von Schmalensee et al., 2024). Ultimately, in this hypothetical relationship between diapause development and temperature, temperatures closer to the thermal maximum will result in shorter diapause durations.

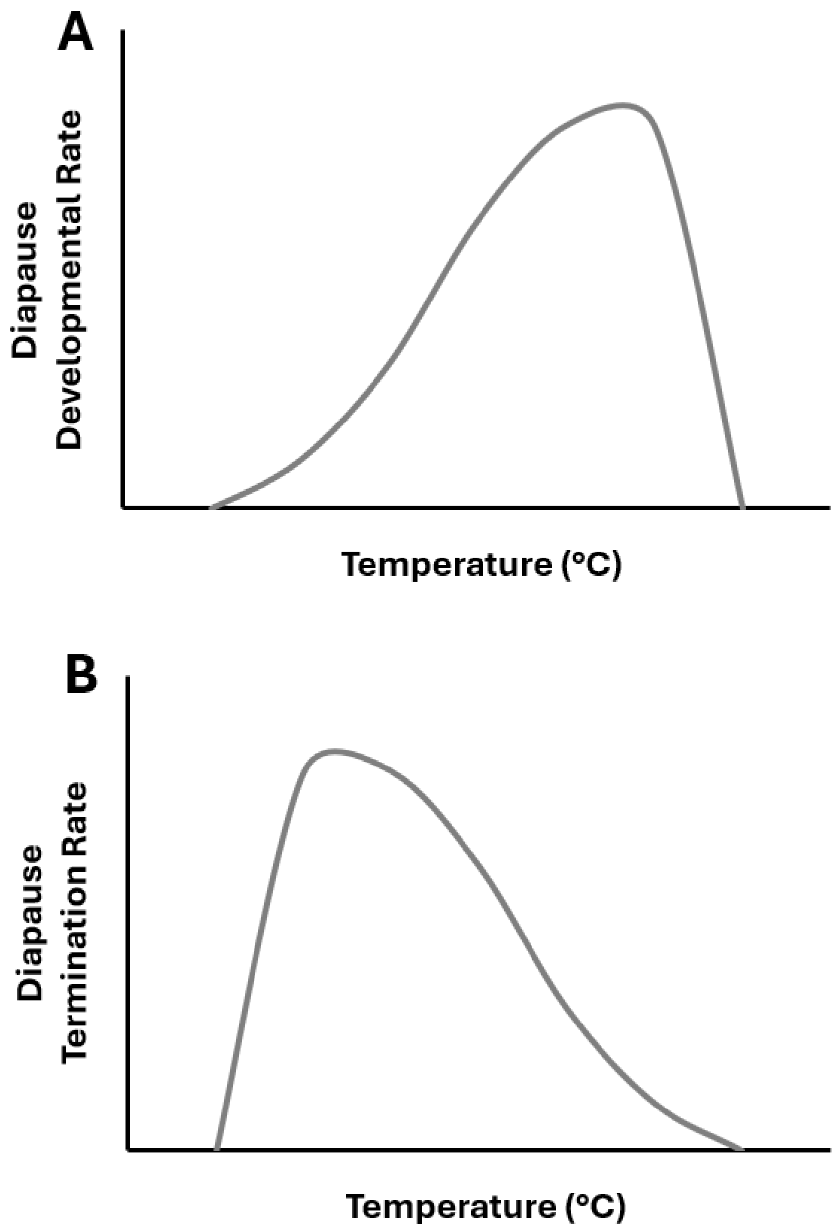

Figure 1.1. Thermal performance curves modeling a hypothetical relationship between diapause developmental rate and temperature. **A**) A typically shaped thermal performance curve, adapted from Toxopeus et al. (2024). **B)** A right-skewed thermal performance curve, based on diapause termination in *P. napi* from von Schmalensee et al. (2024).

The Physiology of Diapause

Hormonal signalling is important for regulating diapause entry and progression through the phases of diapause (Hahn & Denlinger, 2011). While different insect species and life stages employ various pathways to regulate diapause, ecdysteroid and juvenile hormone signalling are the most frequently studied. During morphogenesis, the neuropeptide prothoracicotropic hormone (PTTH) stimulates the insect's prothoracic glands, which in turn releases ecdysteroids that promote molting (Li et al., 2018). In several moth species (Ahmadi et al., 2021; Liao et al., 2024; Süess et al., 2022; Suang et al., 2017), ecdysteroid sensitivity increases during diapause initiation and termination, or the transitional phases between morphogenesis and diapause development. As daylength shortens in fall, sugar beet moth (*Scrobipalpa ocellatella*) pupae detect photoperiodic signals, in turn decreasing PTTH levels and inducing diapause, likely due to decreased ecdysteroid concentrations (Ahmadi et al., 2021). Conversely, increased ecdysteroids leads to diapause termination in bamboo borer (*Omphisa fuscidentalis*) larvae (Suang et al., 2017). Juvenile hormones may also mediate diapause, as observed in the adult mosquito *Culex pipiens* (Sim & Denlinger, 2008). Juvenile hormone concentrations are low during adult diapause maintenance, but increase post-diapause in response to increased insulin. In concert with insulin signalling, the Target of Rapamycin (TOR) pathway and corresponding cell growth hormones are similarly repressed in diapause (Hahn & Denlinger, 2011; Torson et al., 2023).

Since insects do not eat for extended periods of time during dormancy, energy previously funneled into growth and reproduction is instead conserved in storage or used for stress tolerance mechanisms (Sokolova, 2013). Energy reserves consist of substrates stored prior to diapause, such as lipid or carbohydrate storages (Hahn & Denlinger, 2011). Mosquito larvae like *Aedes albopictus*, which undergo facultative diapause in response to photoperiodic cues at the eggs stage, increase their lipid storage by 30% prior to diapause (Reynolds et al., 2012). Conversion of lipids to ATP can aid survival in the absence of foraging during the winter months. Alternatively, cryoprotective metabolites—such as glycerol, sugars like trehalose, and some amino acids—may be accumulated and used to counteract injuries during cold exposures (Hahn & Denlinger, 2011; Overgaard & MacMillan, 2017).

Gene Expression in Diapause

As the diapause program progresses, the insect's gene expression changes across developmental phases and over time, as shown in many transcriptomic studies (Košťál, 2006). In *C. costata* larvae, differentially expressed genes cluster into distinct phases corresponding to diapause initiation, maintenance, and photoperiodic or cold-acclimated termination (Košťál et al., 2017). However, while *C. costata* demonstrates some clear transcriptomic signatures, diapause phases are not necessarily detected as distinctly in every species. In diapausing *R. pomonella*, transcriptomic changes instead occur incrementally, where patterns of expression can be grouped into gene clusters that show steady increases or decreases over the course of six overwintering months (Dowle et al., 2020). Furthermore, gene expression can be clustered into different patterns before, during, and after diapause, as demonstrated by the Asian longhorn beetle, *Anoplophora glabripennis* (Torson et al., 2023). In larval *A. glabripennis*, a particular subset of genes increases their expression from pre-diapause to diapause maintenance, then decreases from diapause to post-diapause development, or vice versa (decreases then increases). Other *A. glabripennis* gene clusters follow the same trajectories but during quiescence instead of diapause (Torson et al., 2023). Increased expression of ecdysteroid-related genes also marks the transition between diapause and quiescence in the alfalfa leafcutting bee, *Megachile rotundata* (Yocum et al., 2015).

To conserve energy in anticipation of challenging seasonal environments, diapausing insects use certain genes and pathways to suppress their metabolism and mobilize energy reserves (Hahn & Denlinger, 2011). Prior to diapause, several insects increase their lipid reserves through regulation of the insulin pathway, of which the downstream *forkhead box O transcription factor* (*FoxO*) gene is often implicated (Sim & Denlinger, 2008; Chen et al., 2024). For example, in the absence of insulin-like peptides, *C. pipiens* upregulate *FoxO* to increase their lipid reserves (Sim & Denlinger, 2008). In addition to sequestering reserves, the gene expression of enzymes that break down fats and carbohydrates tend to be inhibited, further depressing metabolic activity (Hahn & Denlinger, 2011). In an alternate strategy, the Colorado potato beetle, *Leptinotarsa decemlineata*, reduces metabolic activity by breaking down flight muscle mitochondria through the upregulation of the mitophagy-promoting *Parkin* gene (Lebenzon et al., 2022).

Diapausing insects may also minimize energy needs by suppressing growth and arresting cell cycle progression, which they achieve through the regulation of a number of genetic pathways (Koštál, 2006). Cell cycle arrest is exemplified by *C. costata* in its downregulation of the *proliferating cell nuclear antigen* (*PCNA*) gene, preventing DNA synthesis (Koštál et al., 2009). The European corn borer moth, *Ostrinia fuscidentalis*, resume gene expression of cell cycle-related activities upon termination of its larval diapause (Wadsworth & Dopman, 2015). However, differences in seasonal timing exist, where moths with an early diapause termination upregulate *PCNA* after one day in long-day diapause-terminating conditions, whereas late terminators do not (Wadsworth & Dopman, 2015). Cell cycle arrest may also vary between tissues, as demonstrated in gene expression of components of the Wnt pathway, which regulates cell proliferation (Hahn & Denlinger, 2011). Some genes of the Wnt pathway decreased expression during diapause in the Malpighian tubules and midgut of *A. glabripennis* but increased in the brain and fat body, although other Wnt-related processes decreased across tissues (Torson et al., 2023).

Overwintering insects in diapause encounter cold temperatures that can result in chill and/or freeze injury, and preparations or responses to such stressors may be expressed as part of diapause development (Hahn & Denlinger, 2011). Diapausing *A. glabripennis* upregulate various heat shock proteins (HSPs), molecular chaperones that protect proteins under temperature stress (Torson et al., 2023). Changes in gene expression or activity of key metabolic enzymes can facilitate accumulation of cryoprotective molecules such as sugars and alcohols from glycogen stores (Overgaard & MacMillan, 2017; Hahn & Denlinger, 2011). These cryoprotective metabolites may later be used for energy once the risk of freezing has passed, as seen in the domestic silk moth (*Bombyx mori*), which increases gene expression related to glycerol kinases after termination of its embryonic diapause at 5 °C (Kihara et al., 2009). Several species differentially express genes related to the cytoskeleton (Yocum et al., 2015; Lebenzon et al., 2021; Poupardin et al., 2015), which may facilitate cytoskeletal remodeling that helps maintain cell structure integrity. Khapra beetle (*Trogoderma granarium*) larvae express higher levels of antifreeze protein (AFP) transcripts during a 1-week pre-diapause period (25 °C) relative to the following 9-

week diapause period, where larvae were acclimated from 20 °C to 5 °C (Dageri et al., 2023). In *C. pipiens*, gene expression of antioxidants like catalase and superoxide-dismutase-2 increases during diapause, and suppression of this gene expression lowered mosquito survival (Sim & Denlinger, 2011).

The Eastern Spruce Budworm (*Choristoneura fumiferana*)

The eastern spruce budworm is a moth species endemic to North America, where its distribution coincides with the spruce-fir forests that larvae feed on (Marshall & Roe, 2021). Three genetically distinct populations have been described, with restrictions in gene flow linked to the historical glaciers, westerly winds, or mountain ranges separating the Western, Central, and Eastern subpopulations (Lumley et al., 2020). The Western population includes Alaska and Yukon, the Central stretches from southeast Yukon to Manitoba, and the Eastern from Ontario to the Atlantic, with some populations spilling across the Canada-US border and into West Virginia (Lumley et al., 2020). Phenotypic differences exist between populations. For example, northern populations lay fewer but larger eggs to cope with colder climates, while the inverse is true for southern populations (Harvey, 1983). However, many studies—including this thesis—have been based on a laboratory colony maintained at the Great Lakes Forestry Centre (GLFC, Natural Resources Canada, Canadian Forest Service) in Sault Ste. Marie, Ontario, Canada. The spruce budworm laboratory colony was sourced from multiple locations in Ontario during the 1960s, and 30+ generations have been documented since quality control implementations in 2006 (Roe et al., 2018).

Throughout its life cycle, the spruce budworm experiences egg, larval, pupal, and adult stages. After hatching from their eggs in late summer or early fall, larvae undergo six different developmental stages known as instars (Marshall & Roe, 2021). Individual larval instars are characterized over six stages where each number (L1-6) represents a phase with specific physical and developmental features. As L1s, budworm exhibit wandering behaviours, as they seek out shelter in the lower tree crowns suitable for overwintering. Here, they construct a hibernaculum; a silk structure which helps protect them during winter, although its exact function remains unknown (Harvey, 1957). Within the hibernaculum, larvae shed their headcaps and expel their gut contents, molting from L1 to L2, and continue spinning behaviors in preparation for diapause. During the first two instars, larvae do not feed, sustained only by maternal energy from the egg reserves (Marshall & Roe, 2021). Additionally, the gene expression of two proteins—*Choristoneura fumiferana* diapause associated proteins 1 and 2 (*Cf*DAP1 and 2)—increase during the first two instars and remain high throughout winter (Palli et al., 1998). Lipid reserves remain stable during overwintering as well (Han & Bauce, 1993). In the spring, post-diapause L2s then emerge from their hibernacula (Marshall & Roe, 2021). At this point, they start feeding on a diet of mainly white spruce (*Picea glauca*) and balsam fir (*Abies balsamea*) needles. During the spring and summer months, they will progress from the L2 stage through L6. When reared at constant 20 °C, pupation will occur 3 weeks post-diapause (GLFC, 2015). *Cf*DAP1 and 2 reappear in the budworm's gene expression during pupation, suggesting a function during non-feeding stages (Palli et al., 1998). If continually reared at 20 °C, the spruce budworm emerges as an adult moth about a week later, which will mate, lay eggs, and begin the cycle anew (GLFC, 2015).

While L2 budworm remain in a functionally obligate diapause state overwinter, variations do exist within the diapause phenotype (Marshall & Roe, 2021). There is a less common non-diapause population of budworm which does not diapause at all, instead vacating their hibernaculum early and continuing morphogenesis (Harvey, 1957). This non-diapause phenotype has been documented in laboratory settings, seemingly in response to longer daylengths (Harvey et al., 1957; van der Burg et al., 2024). On the other end of the spectrum, some budworm have a two-year life cycle and diapause twice rather than once. Two-year budworm occur in western Canada and undergo two winter diapauses at different larval instars, where the second diapause is during the fourth instar (Harvey, 1961). This is akin to the western spruce budworm, *Choristoneura biennis*, of the same genus and from a similar region, which undergoes two winter diapauses: one obligate followed by a facultative (Harvey, 1967).

Successful overwintering facilitates spring budworm emergence, which, during cyclical outbreaks, may occur en masse (Marshall & Roe, 2021). Outbreaks oscillate at 30- to 40-year intervals, and the budworm's capacity for defoliation during these times is of particular concern to forestry and pest managers. To illustrate, the 1979-1987 outbreak in Nova Scotia affected 2.5 million hectares of land (Sponagle, 2022). Future Canadian outbreaks are projected to lead to losses in the forestry industry ranging from millions to billions of dollars (Liu et al., 2019). To combat the budworm's economic impact, forestry managers in New Brunswick have implemented a control method called the Early Intervention Strategy (EIS), with promising results (MacLean et al., 2019). By assessing L2 overwintering density, the EIS framework detects population hotspots in the early stages of an outbreak and uses that information to determine best management practices.

As such, understanding the biological processes underlying diapause timing and duration may help inform and optimize the implementation of EIS and other pesticide programs.

Temperature Effects on Budworm Diapause

In the face of climate change, the interactions between changing temperatures and diapause development in insects like the spruce budworm remain of scientific interest (Denlinger, 2023). To adjust to changing climates, insects may shift their population distribution to remain within preferred temperature ranges (Marshall et al., 2020). In the case of *C. fumiferana*, this forest pest is likely to adapt to new host species, such as black spruce (*Picea mariana*), if temperatures north of their current distribution become permissive (Bellemin-Noël et al., 2021). Shifting population ranges and increased gene flow between populations may also allow for increased egg clutches in northwestern habitats, putting these areas at higher risks for outbreaks (Lumley et al., 2020). However, while future winters may become warmer, they may also include more extreme cold events that could influence the evolution of insect cold hardiness and the timing of lifecycle events such as diapause entry and spring emergence (Marshall et al., 2020).

Like many other diapausing insects, *C. fumiferana* employs a suite of cold tolerance mechanisms to survive winter, both lowering their temperature threshold of internal freezing and increasing production of cryoprotective molecules (Marshall & Roe, 2021). Historically, between 1961 and 1990, Ontario populations lived through average winter temperatures ranging from -22.6 °C to -11.2 °C (Candau & Fleming, 2008). Impressively, *C. fumiferana* may briefly survive temperatures as low as -36 °C before internal freezing occurs (Marshall & Roe, 2021). Another protein group, AFPs, which inhibit the development of ice within an insect's body by binding to ice crystals, are expressed in the L1 and early L2 stages of *C. fumiferana* (Béliveau et al., 2022). Cryoprotective molecules like glycerol further depress the budworm's temperature of internal freezing (Butterson et al., 2021). During the overwintering period, glycogen reserves decrease as glycerol increases (Han & Bauce, 1993). Diapausing spruce budworm can express multiple distinct small HSPs (Quan et al., 2018a-b), which may protect proteins during cold exposure (Overgaard & MacMillan, 2017).

Warm pre-winter temperatures appear to influence overwintering survival, suggesting that temperature exposures could influence the budworm's ability to successfully complete diapause processes. Lab-reared first-instars exposed to longer, warmer field conditions (July/August) prior to winter exhibit poorer post-winter survival than those exposed to cooler field conditions (September/October) (Han & Bauce, 2002). A more recent study showed a similar result, where long warm (20 °C) pre-winter conditions in the lab resulted in glycogen depletion and poor overwintering survival (Roe et al., 2024). Long, warm falls at 20 °C corresponded with lower glycogen content, suggesting that energy depletion increased mortality by starvation. Larvae exposed to a short, cool fall at 10 °C had significantly higher glycogen content compared to the long, warm fall group, but their overwintering survival remained similarly low. While larvae in long, cool falls had lower glycogen content than the short, cool fall group, their survival was highest (Roe et al., 2024). If diapause is a temperature-dependent process in *R. pomonella* and *P. napi* (Toxopeus et al., 2024; von Schmalensee et al., 2024), low overwintering survival in *C. fumiferana* could suggest that a temperature-requirement needs to be met during fall before larvae can successfully initiate and complete diapause (Roe et al., 2024).

The Function of the Hibernaculum

Several insects construct cocoons or hibernacula as shelter during overwintering, including spruce budworm, possibly aiding overwintering survival in different ways (Danks, 2004; Marshall & Roe, 2021). In preparation for overwintering, first-instar budworm construct the first layer of the hibernacula, wherein they molt into second-instar larvae, which continue spinning behaviours and may construct a second layer (Harvey, 1957). A double-layered structure has been suggested to improve protection against inoculative freezing and other environmental threats, and possibly alter photoperiodic cues (Danks, 2004). Non-diapausing first-instar budworm may also construct a hibernaculum but evacuate it after molting, and some non-diapausing larvae bypass hibernaculum construction entirely (Harvey, 1957). While it has been speculated that the hibernaculum may increase *C. fumiferana* desiccation (drying) resistance, larvae that remained within or were removed from their hibernacula experienced similar levels of water loss after two weeks (18 °C) of desiccant exposure (Han & Bauce, 2001). Other lepidopteran larvae, such as the Glanville fritillary butterfly (*Melitaea cinxia*) and the Arctic woolly bear moth (*Gynaephora groenlandica*), use silk as a barrier against pathogens and parasitoids during winter or summer, respectively (Duplouy et al., 2018; Kukal, 1995). The silk of *B. mori* also has antimicrobial properties (Singh et al., 2014; Dong et al., 2023), which could translate to improved stress tolerance for overwintering budworm. So, although the hibernaculum likely provides a shelter that is important for spruce budworm during overwintering, the exact biological mechanisms of which it may aid budworm survival has yet to be articulated in current research.

Research Objectives

For my M.Sc. project, I assessed how fall temperatures impact budworm diapause and associated key biological processes. To accomplish this, I performed a time-series experiment, exposing the budworm to either warm or cool simulated fall conditions for ten weeks and then compared these two treatments to better understand potential temperature-driven influences. I hypothesized that an unknown temperature-sensitive process occurs during the beginning of budworm diapause. I predicted that this process completes later in cool fall conditions and earlier in warm fall conditions, resulting in gene expression following one or more of the trajectories illustrated in Fig. 1.2. A cool fall will cause expression of this trait at a more gradual rate, and—based on optimal survival in the Roe et al. (2024) study—complete after approximately 7 weeks (Fig. 1.2). Based on the same data, larvae in a warm fall will complete this process after approximately 2 weeks (Fig. 1.2). Once the temperature-dependent process has completed at either 2 or 7 weeks, the expression of this trait could either continue to increase, plateau, or decrease (Fig. 1.2). Multiple genes may be differentially expressed between warm and cool fall conditions, and I have listed several candidates that I expect to be involved in diapause progression based on other Lepidoptera and larval diapausers (Table 1.1).

As the methodology for measuring budworm gene expression required the removal of hibernacula, a new question arose about the function of the hibernaculum and how its absence could influence gene expression. Consequently, I performed an additional fall and winter time series to assess the impacts of hibernaculum removal on the budworm's overwintering survival. I hypothesized that the hibernaculum increases spruce budworm overwintering survival. I further predicted that larva that remained without hibernaculum from the beginning of fall and throughout winter would have lower motility and post-winter dispersal than budworm that remained in hibernacula throughout fall and winter or had their hibernacula removed midway through the time series. Of the latter two treatments, I predicted larva that always remained in hibernacula to have the highest motility and post-winter dispersal.

Ultimately, my research will fill in the literature gap on the physiological mechanisms of early budworm diapause. After identifying any instrumental biological processes that take place during the fall simulations, I may be able to relate them to the initiation phase of diapause in spruce budworm, which helps predict the total duration of diapause. Such an understanding of budworm diapause will also improve the timing of programs like EIS (MacLean et al., 2019), helping pest and forestry managers better predict spruce budworm emergence and outbreaks in relation to fall temperatures in variable future climates (Marshall et al., 2020).

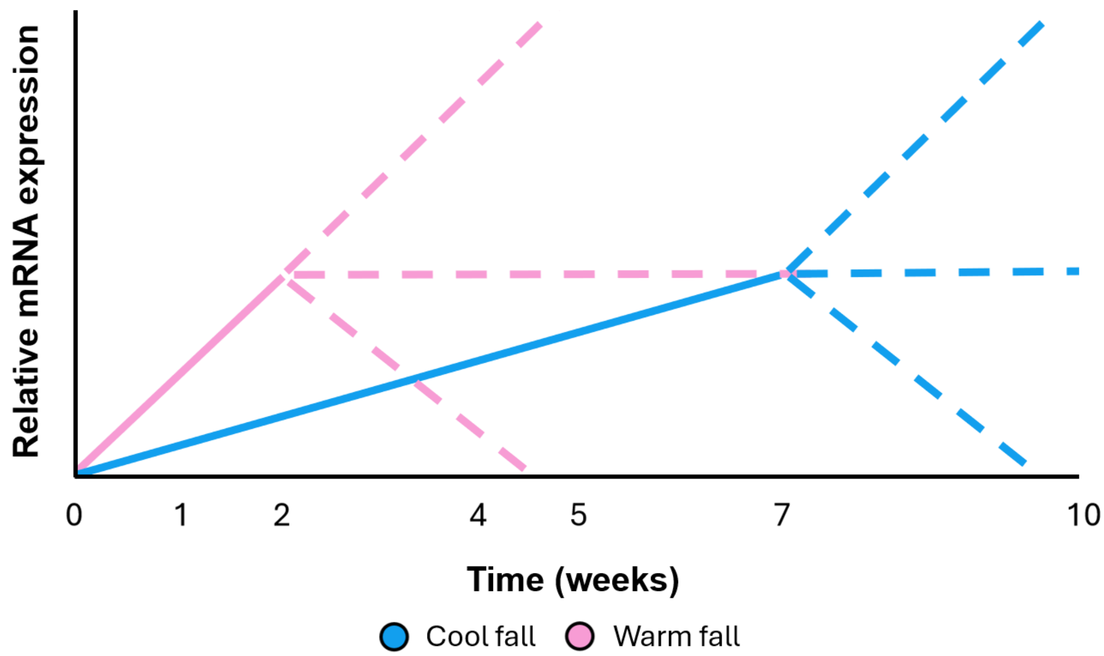

Figure 1.2. Predicted relative mRNA expression of a gene supporting an unknown temperature-dependent diapause process in *C. fumiferana* during a cool (blue) or warm (pink) 10-week fall treatment. Solid lines indicate initial increase or decrease of mRNA expression, and dashed lines indicate possible trajectories (increase, plateau, decrease) after a hypothesized temperature requirement is met.

Table 1.1. Predicted candidate genes that support temperature-dependent progression of early diapause in *C. fumiferana*. Arrows (↓ or ↑) signal their expected increased or decreased gene expression, which would occur earlier in a warm fall, and later in a cool fall. Candidate genes were selected from literature featuring species that are either lepidopteran and/or undergo diapause in the larval stage.

Diapause Phenotype	Gene or Process	Species	Order	Life Stage	Reference(s)
Arrested development	↓ *PCNA*	*Chymomyza costata*	Diptera	Larva	Koštál et al., 2009; Poupardin et al., 2015
Arrested development	↓ Wnt processes	*Anoplophora glabripennis*	Coleoptera	Larva	Torson et al., 2023
Arrested development	↑ Clock genes (*Per* & *Tim*) ↓ PTTH	*Scrobipalpa ocellatella*	Lepidoptera	Pupa	Ahmadi et al., 2021
Arrested development	↑ Photoreception	*Choristoneura fumiferana*	Lepidoptera	Larva	van der Burg et al., 2024
Arrested development	↓ 20-hydroxyecdysone ↓ *HR3*	*Pieris rapae*	Lepidoptera	Pupa	Liao et al., 2024
Metabolic restructuring	↓ Insulin growth factor processes	*Ostrinia nubilalis*	Lepidoptera	Larva	Wadsworth & Dopman, 2015
Metabolic restructuring	↑ *Cf*DAP1 & 2	*Choristoneura fumiferana*	Lepidoptera	Larva	Palli et al., 1997
Metabolic restructuring	↓ Lipid catabolism	*Aedes albopictus*	Diptera	Larva	Reynolds et al., 2012
Stress tolerance	↑ *Cf*AFPs	*Choristoneura fumiferana*	Lepidoptera	Larva	Béliveau et al., 2022
Stress tolerance	↑ *Cf*HSP22.0	*Choristoneura fumiferana*	Lepidoptera	Larva	Quan et al., 2018
Stress tolerance	↑ Glycerol & glycogen synthesis	*Choristoneura fumiferana*	Lepidoptera	Larva	Han & Bauce, 1998

Table 1.1. continued.

Diapause Phenotype	Gene or Process	Species	Order	Life Stage	Reference(s)
Stress tolerance	↑ Fatty acid membrane remodelling	*Aedes albopictus*	Diptera	Larva	Reynolds et al., 2012
Stress tolerance	↑ Superoxide dismutase	*Antheraea mylitta*	Lepidoptera	Pupa	Sahoo et al., 2018
Stress tolerance	↑ Glutathione S-transferase (antioxidant)	*Helicoverpa armigera*	Lepidoptera	Pupa	Zhang et al., 2013

Chapter 2: Methods

Insect Colony & Rearing

The spruce budworm larvae for my project were supplied by the Insect Production and Quarantine Laboratories (IPQL) at the GLFC. Since the 1960s, the IPQL has reared spruce budworm of mixed Ontario origin, currently consisting of 16 lab-adapted families (Roe et al., 2018). At the IPQL, budworm eggs of the generation F32 from IPQL family number 10 (*Cf*10-F_{32}) were placed in controlled environmental conditions (23±3 °C, 16:8 h Light:Dark, and 55±10% relative humidity; GLFC, 2015). After approximately two weeks, the hatched second instar larvae (L2) were transferred to overwintering conditions (2±3 °C, 0:24 h Light:Dark, and 55±10% relative humidity) for approximately 21 weeks (150 days) or 25 weeks (178 days). 21-25 weeks of overwintering conditions are within IPQL larvae's window for optimal overwintering survival and post-winter rearing (GLFC, 2015). Following overwintering, the IPQL returned budworm larvae to original hatching conditions and reared them on a synthetic agar-based diet (McMorran, 1965). Larvae progressed from second through sixth instars and matured into pupae ca. 25 days after overwintering (GLFC, 2015), at which point they were shipped at ambient temperature to the Toxopeus lab at St. Francis Xavier (St. FX) University in Antigonish, NS, Canada.

I received pupae of the generation *Cf*10-F_{32} in two separate shipments to the Toxopeus lab. The first pupae (from larvae with 21 weeks overwinter) were mailed from Sault Ste. Marie on August 26, 2024, and arrived in Antigonish on August 29, 2024. The second shipment (from larvae with 25 weeks overwinter) was sent September 24, 2024, and arrived September 26, 2024. Pupae were shipped in plastic containers cushioned with paper towels. I used budworm from the short winter group (first shipment) for the transcriptomic experiment, and budworm from the long winter group (second shipment) for survival data and an additional experiment exploring the effects of hibernaculum removal, described in later sections.

After arriving to St. FX, pupae were reared to adulthood according to the IPQL standard operating procedure, with slight modifications (GLFC, 2015). During rearing, *C. fumiferana* were maintained at 23±3 °C, 16:8 h Light:Dark, and 20–60% relative humidity unless described otherwise, and kept in either a temperature-controlled room in the St. FX Animal Care facility or an MIR-154 incubator (PHCbi, Wood Dale, IL, USA). First, I transferred pupae into eclosion chambers separated by sex. 15 L plastic containers with a fine metal mesh cut-out lid (allowing air circulation) were disinfected with 70% ethanol and lined with paper towels on the bottom of the container and over the cut-out (preventing escape) to house eclosing pupae (Fig. 2.1A). The pupae eclosed into mature moths within 0 to 5 days of arrival, and eclosion chambers were misted with distilled water daily until transfer to mating chambers. I transferred the short winter group to a mating chamber on the fifth day after arriving to St. FX and the long winter group on the third day, the latter of which had more moths and a higher eclosion rate.

Following eclosion, moths were transferred to new chambers for mating (GLFC, 2015). To slow down moth activity during transfer, I cooled them in the eclosion chambers at 4 °C for 5 to 10 min in an MIR-154 incubator. I transferred moths using soft forceps into mating chambers, which consisted of clear plastic bags (Fig. 2.1B). Each mating chamber contained three sets of five wax paper strips stapled together, which were pleated and crumpled to create creases for moths to lay eggs in. Mating chambers were misted with distilled water before moth transfer and every other day until egg harvest. After transferring the moths, I filled the plastic bag with air using either a bike or aquarium pump depending on equipment availability, and secured the bag with a twist tie. The 21-week winter group's mating chamber consisted of 104 female and 99 male moths, while the 25-week winter group consisted of 106 female and 106 male moths. To delay egg-laying for the long winter group so that downstream experimental procedures aligned with the short winter group, I placed their mating chamber in an MIR-154 incubator at 5 °C and 0:24 h Light:Dark, as in Stehr (1954). After two days in cool darkness, I returned this mating chamber to standard rearing conditions (23 °C) in the Animal Care facility room. However, due to overheating of the facility (up to ca. 27 °C), I moved the mating chamber into an incubator for the last three days of the mating period.

Five days after mating started, I harvested *C. fumiferana* eggs and transferred them to pans for hatching (GLFC, 2015). Eggs were first placed in a plastic container set up the same way as the eclosion chambers (Fig. 2.1A), then left to harden. Following a 24-hour period, I disinfected eggs according to the IPQL standard operating procedure, rinsing them with a 1% (v/v) Clorox bleach solution. Wax strips were left to dry at room temperature (ca. 22 °C) for 2-3 hours, hanging by clips from clothes hangers (Fig. 2.1C). I placed dislodged eggs on paper towels on top of a vented metal tray. Once dry, I transferred all eggs to hatching pans with cheesecloth for hibernaculum spinning, as per IPQL procedures (GLFC, 2015). Cheesecloth patches (13 cm × 23 cm) were attached to the bottom of the pan with Parafilm and to the Parafilm covering the top of the pan (Fig. 2.2A). Wax strips and dislodged eggs surrounded the bottom cheesecloth patch. Finally, I enclosed the pan with a cover made of dark blue cardboard (Fig. 2.2B). The cover had a cutout (ca. 12 cm ×

10.5 cm) allowing light to shed onto the cheesecloth patches, encouraging hatched budworm to move toward the cheesecloth. The budworm were given 12 days in standard rearing conditions to hatch into first-instar larvae, which then wandered in search of overwintering sites, establishing hibernacula in the cheesecloth. Following hibernaculum spinning, first-instar larvae molted into second-instar larvae (still within their hibernacula), which were used in experiments described in the next sections.

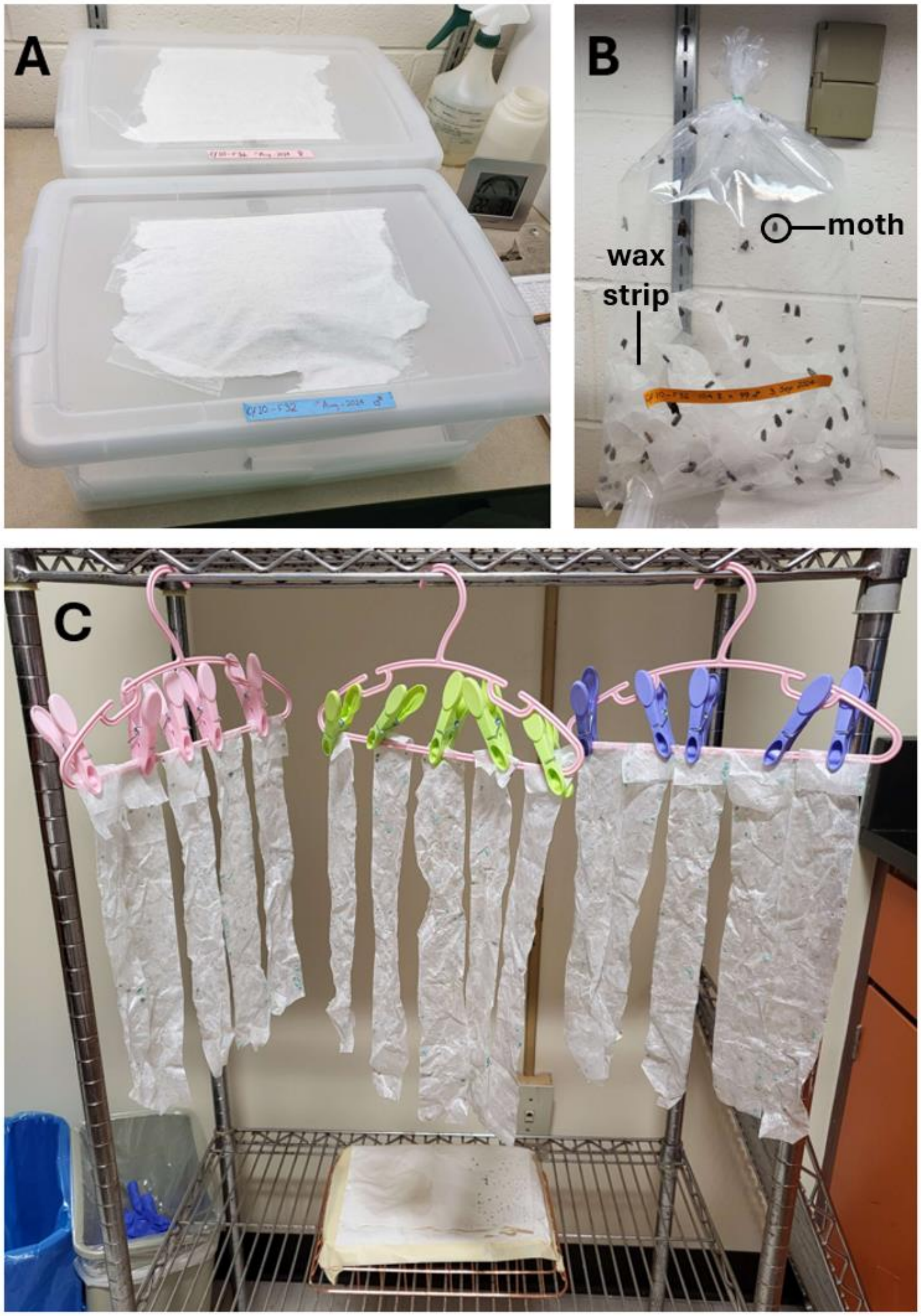

Figure 2.1. Rearing set-up and egg harvest of *Cf*10-F$_{32}$. **A)** Eclosion chambers, consisting of plastic containers with a mesh opening covered in paper towels, used to house eclosing pupae. **B)** Mating chambers, consisting of plastic bags containing wax strips for egg-laying, which contained approximately 100 moths of each sex. Lines point out moth and wax strips. **C)** Clothes hangers and clips used for drying disinfected wax strips, and a vented metal tray blanketed with paper towels for drying dislodged eggs below. Blue clusters on strips and paper towels are egg masses.

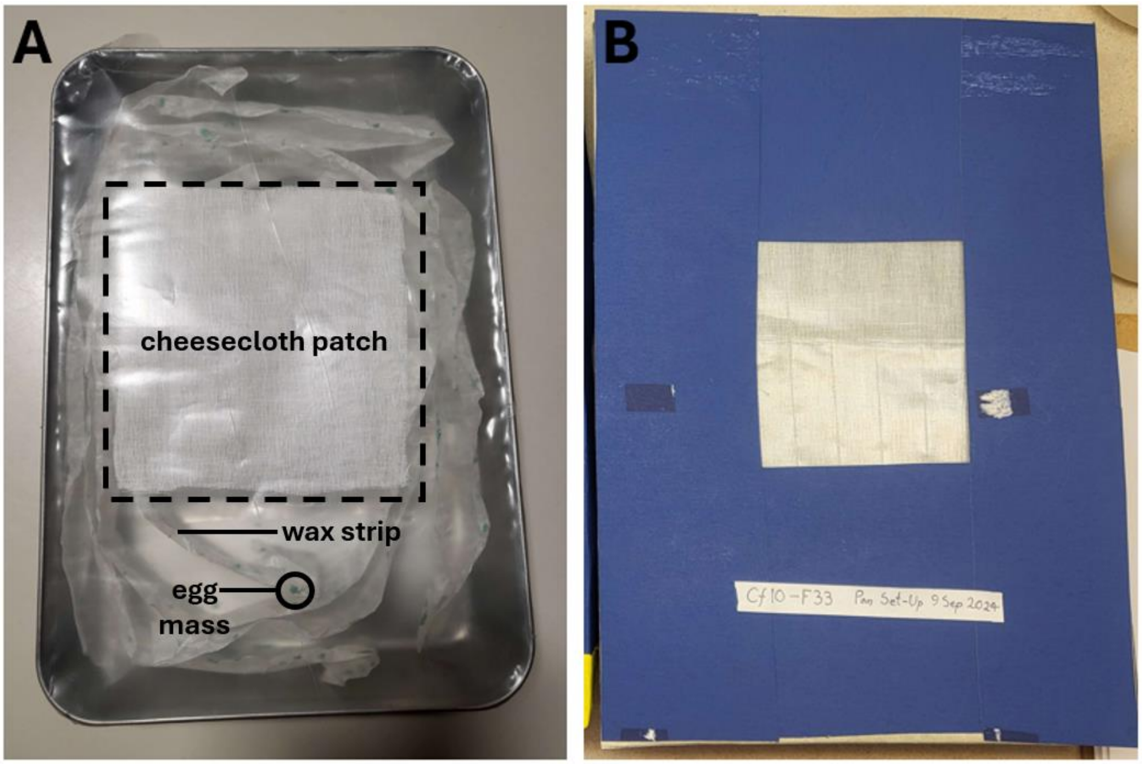

Figure 2.2. Hatching pans for L2 emergence of *Cf*10-F$_{33}$. **A)** Hatching pan enclosed with Parafilm, containing cheesecloth patches on both Parafilm and bottom of pan, with wax strips containing eggs surrounding the cheesecloth. Cheesecloth patches are framed with dashed lines, and solid lines point to a wax strip and egg mass. **B)** Hatching pan enclosed with a dark blue cardboard lid above Parafilm, with a cutout for light access above cheesecloth patches.

Fall Time Series Transcriptome & Motility

Experimental Design

To learn more about diapause gene expression in budworm, I exposed L2s to either a cool (10 °C) or warm (20 °C) simulated fall for 10 weeks and a photoperiod of 16:8 h Light:Dark at 20–50% relative humidity (Fig. 2.3). The simulation started on September 22, 2024 and concluded on December 1, 2024, spanning timepoints 00-07 (Table 2.1). Timepoint 00 represented a control group of budworm at the start of the experiment, one day following hibernaculum removal (see below) at room temperature (ca. 22 °C). Budworm associated with timepoints 01-07 were treated with either a cool or warm fall for different durations (2 days to 10 weeks) one day following hibernaculum removal. Durations and temperature were chosen based on survival results in Roe et al. (2024), within the window of time where larvae exposed to either warm and cool fall temperatures reach optimal overwintering survival. At each timepoint, I removed a group of budworm from experimental conditions to capture transcriptomic signatures at the given time. A timepoint included five biological replicates for later RNA extractions (Table 2.1). Each replicate contained 50 budworm that were pooled due to their small size, which ensured detection of RNA. At several timepoints, one additional biological replicate was also used to assess larval motility as a proxy for survival, as described in the hibernaculum removal section.

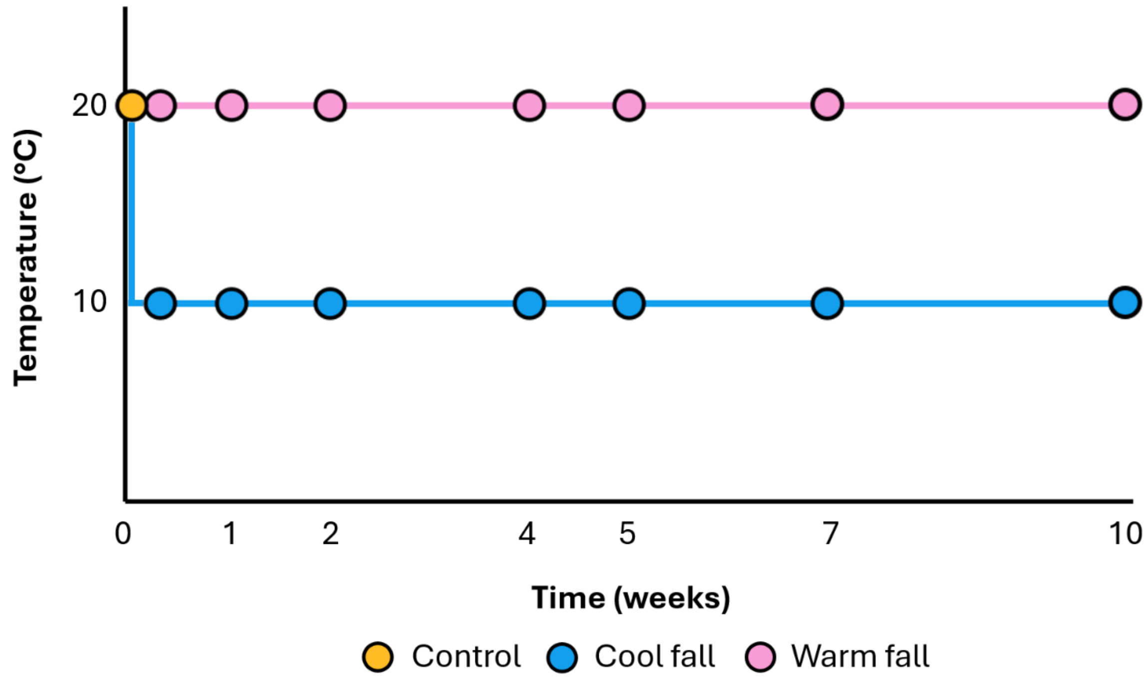

Figure 2.3. Temperature regime for a cool or (10 °C) or warm (20 °C) fall treatment across 10 weeks for transcriptomic analysis of *C. fumiferana* larvae. Pink represents the warm fall treatment, blue represents the cool fall treatment, and orange represents a control group maintained at room temperature (ca. 22 °C). Each timepoint included 3-5 replicates for RNA sequencing and 1 replicate for motility assessment. Larvae were maintained at 16:8 h Light:Dark at their respective fall temperature treatment.

Table 2.1. Fall length for each budworm group (00-07) in the fall transcriptome and motility experiment. Timepoints include a control (00) at room temperature (ca. 22 °C) while subsequent timepoints (01-07) were exposed to either cool (10 °C) or warm (20 °C) simulated fall conditions (16:8 h Light:Dark and 20-50% relative humidity).

Timepoint	Time in fall conditions
00	0 days
01	2 days
02	1 week
03	2 weeks
04	4 weeks
05	5 weeks
06	7 weeks
07	10 weeks

Experimental Set-Up

Upon reaching their 2nd larval instar, the developmental stage at which *C. fumiferana* undergoes diapause, I removed larvae from their rearing conditions inside the hatching pans. Larvae were removed from cheesecloth by parting the cloth from its Parafilm. As parting the cheesecloth often broke the hibernacula, larvae were allowed to either crawl or fall onto a paper towel surface. If the hibernaculum remained intact after separating the cheesecloth, I carefully parted it open with fine-tipped forceps to reach the larva. I then used a paintbrush to gently move larvae into FisherBrand 1.5 mL microcentrifuge tubes (Thermo Fisher Scientific, Mississauga, ON, Canada) with perforated screw caps, each tube housing 50 budworm that amounted to one biological replicate for later RNA extractions. The cap was carefully screwed on top of a paper stopper (2.5×2.5 cm paper towel piece) which prevented budworm from escaping through the cap perforations, while also allowing air to permeate the tube. All handling prior to incubation occurred at room temperature (ca. 22 °C). Transferring larvae into tubes occurred within a day (approximately 10 hours). The following day, all experimental larvae were haphazardly assigned a fall treatment and time, and simultaneously moved into MIR-154 incubators (PHCbi, Wood Dale, IL, USA) for their respective fall treatment (Table 2.1), except for timepoint 00. I followed the same procedure at a later date for corresponding motility assessments using offspring from the second pupae shipment.

Motility & Survival Assessment

As a proxy for survival, I measured the motility of budworm across timepoints 00-07 (Table 2.1). I classified budworm as motile or immobile, which I then further subcategorized (Fig. 2.4). Using a paintbrush, I gently moved budworm from their tube onto a paper towel, and observed them under a dissecting scope. Motile budworm (Fig. 2.4A) varied in their ability to move, ranging from actively crawling to subtle limb movements visible once flipped on their back. Immobile budworm (Fig. 2.4B-F) displayed no movement, whether unprompted or gently prodded with a paintbrush. Ensnared larvae occasionally occurred in tubes where budworm had been removed from their hibernacula, as spinning of new hibernaculum threads led to entanglements (Fig. 2.5B). If larvae were still motile within these entanglements, they were classified as such. Some L2s were classified as shrunken in appearance, which could occur to varying degrees and was associated with a darker brown body colour (Fig. 2.5C-D). L2s appeared shrunk like Fig. 2.5C, but curled were classified as shriveled appearance, potentially dehydrated (Fig. 2.5E). Immobile L1s never progressed to L2s, as indicated by the visible gut content which L2s usually evacuate (Fig. 2.5F). Larvae that appeared contorted in some way other than the aforementioned categories, perhaps due to reasons such as molting failures or handling injuries, were classified as deformed.

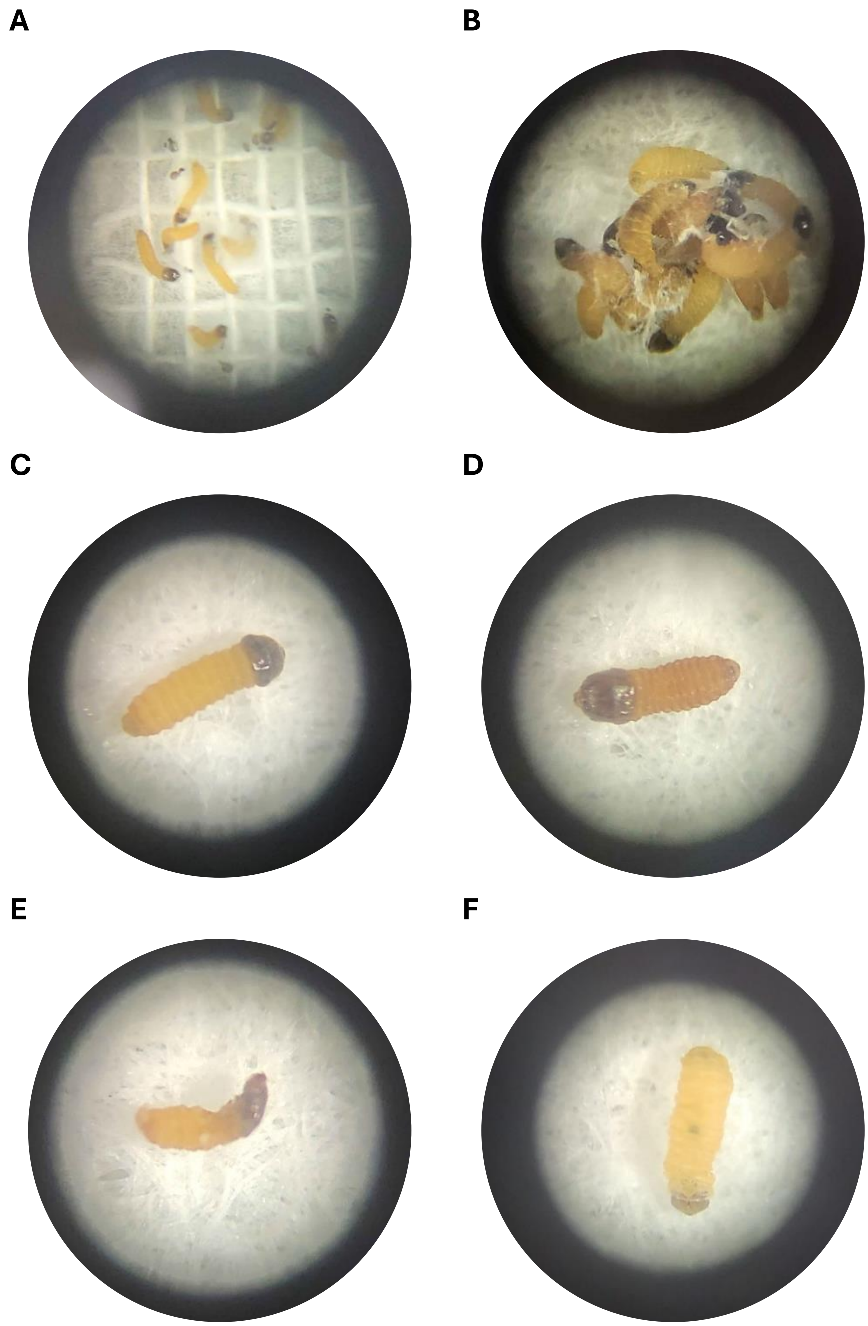

Figure 2.4. (A) Motile and **(B-E)** immobile budworm larvae during diapause, as observed through a dissecting microscope ocular lens. **A)** Motile larvae on a cheesecloth patch. **B)** Larvae ensnared in hibernaculum threads after hibernaculum removal and tube transfer. **C-D)** Immobile L2s with varying degrees of a shrunken appearance relative to motile larvae in A. **E)** Immobile L2 with a shrunken but curled up body, as if "shriveled" in appearance. **F)** Immobile L1 that never progressed to L2 and retained its gut contents, visible as a green speck.

RNA Extraction, Library Preparation, & Sequencing

At each timepoint (Fig. 2.3; Table 2.1), I flash-froze 5 tubes from the control (timepoint 00) or each of the two fall simulations (timepoints 01-07) in the morning, then stored them in a –80 °C freezer until RNA extraction. Later, some of these replicates were excluded, either due to equipment failure during RNA extraction resulting in spilled RNA or for failing quality control during or after library preparation for RNA sequencing, detailed in this section. Ultimately, each timepoint included 3–5 replicates.

In preparation for RNA extraction of fall time series samples, I removed paper stoppers from each tube, then added 0.09–0.10 g of 0.9–2.0 mm steel beads. In a Bullet Blender Storm Pro (Next Advance, Inc., Troy, NY, USA), I homogenized budworm without (2 min) then with (1 min and 15 s) 500 µL TRIzol reagent (Thermo Fisher Scientific). For homogenization with TRIzol, I reduced the Bullet Blender's speed from 12 to 8 and paused it at 15 s-intervals to tighten screwcaps. Due to TRIzol leakage during homogenization, one sample was lost from timepoint 02 (cool fall) and two from timepoint 03 (warm fall). After transferring liquids to new tubes without beads, I incubated them at room temperature (ca. 22 °C) for 5 min. I added 100 µL of chloroform to the tubes before incubating again for 3 min at room temperature (ca. 22 °C), then centrifuging for 15 min at 12,000 × *g* and 4 °C. Subsequent incubations were on ice, unless specified. I then transferred the upper aqueous liquid layer, which contained extracted RNA, into new tubes. To isolate the RNA from the supernatant, I added 250 µL isopropanol and incubated samples for 10 min and centrifuged for 10 min at 12,000 × *g* and 4 °C. This yielded a pellet containing RNA in each tube. I removed the supernatant and added 500 µL of 75% ethanol which I centrifuged for 5 min at 7,500 × *g*. I then air-dried the ensuing RNA pellet and added 50 µL RNase-free water. To resuspend the RNA in solution, I incubated tubes in a heat block at 60 °C for 15 min. Lastly, I used a NanoDrop One C (Thermo Fisher Scientific) to perform UV spectrophotometry, determining RNA purity and concentration based on absorbance at wavelengths of 230, 260, and 280 nm.

Following RNA extraction, I shipped 72 samples on dry ice to the genomics facility Génome Québec (Montreal, QC, Canada) for quality control and library preparation. Génome Québec used a NEBNext Ultra II library preparation kit (New England Biolabs, Inc., Ipswich, MA, USA) to generate complementary DNA (cDNA) from mRNA in the total RNA extracts. cDNA concentration was quantified using Qubit technology. One sample, associated with the control group, did not pass quality control with a Bioanalyzer. The remaining samples that passed quality control with a Bioanalyzer then underwent library preparation. Sequencing of polyA-enriched RNA libraries were performed with a NovaSeq Illumina platform (Illumina, San Diego, California, USA). The 71 samples were processed on 7 lanes (10 or 11 samples per lane) as 100 bp paired-end reads, at a depth of 32 million reads per sample. This yielded FASTQ files containing sequence data for each read.

Data Processing & Analysis

Prior to data processing, Genome Quebec performed FastQC v0.12.1 (Andrews, 2010) analysis on the raw reads with a MultiQC v1.23 (Ewels et al., 2016) aggregate report to summarize the quality of the sequencing output. I trimmed and removed low quality sequences from the Illumina output with the software Trimmomatic (v0.39; Bolger et al., 2014), using the following operations: ILLUMINACLIP to remove Nextera adapters, LEADING:3 and TRAILING:3 to cut bases off the start or end of the read if below a certain quality, SLIDINGWINDOW:4:15 which trimmed reads based on average quality, and MINLEN:36 to exclude short (i.e., < 36 bp) sequences. Using FastQC again, I assessed sequence quality and identified biological replicates that were potential outliers (one from timepoints warm fall 01 and cool fall 03 each) based on overrepresented sequences before aligning the reads to the *C. fumiferana* genome. I mapped reads with HISAT2 v2.2.1 (Kim et al., 2019) to Béliveau et al.'s (2022) *C. fumiferana* reference genome, accessible through the National Center for Biotechnology Information (NCBI) databases (accession: CM046102). I then generated read counts with HTseq 2.0.9 (Anders et al., 2015), measuring how many copies of transcripts represented each gene within the genome. HTseq counts were normalized in DESeq2 (Love et al., 2014) in R (v4.2.2; R Core Team, 2025) before analysis.

Next, I identified and analyzed genes that were either of interest to budworm diapause or differentially expressed between cool and warm fall simulations. I performed a principal component analysis (PCA) of the treatment groups (time × fall temperature) using R's prcomp function, as described in Torson et al. (2023). I also ranked the top 500 most influential genes—where influence was determined in DESeq2—by their contribution (%) to the principal components. I then used maSigPro v1.70.0 (Conesa & Nueda, 2024) in R to detect gene expression patterns during the 10-week fall simulation. To decipher trends within the resulting clusters of genes, I ran a Gene Ontology (GO) enrichment analysis with the topGO v2.50.0 (Alexa & Rahnenfuhrer, 2022) R package. If significantly enriched genes were annotated < 2 times, these genes were excluded from the GO enrichment analysis. Of 16,231 genes in the reference genome, 8,417 were successfully annotated with GO terms using InterProScan 5 (Jones et al., 2014). Additionally, I completed a targeted search of my genes of interest in both the PCA and maSigPro clusters (Table 1.1). For genes of interest that were not present in the clusters or PCA, I performed linear regression analyses with a Bonferroni correction for multiple analyses. Lastly, I visualized the expression of these genes with ggplot2 v3.5.2 (Wickham, 2016) in R.

Effects of Hibernaculum Removal

Experimental Design #1:

Effect of Hibernaculum Presence on Survival During Fall & Winter

Larvae underwent a fall and winter simulation that lasted from October 21, 2024 until the March 12, 2025. I exposed the experimental groups to a 17-day warm fall at 20 °C and 16:8 h Light:Dark, closely aligned with the IPQL standard operating procedure's pre-diapause duration of 2 weeks (GLFC, 2015). Then I transferred budworm to an 18-week overwintering period at 2 °C in total darkness. Nine timepoints (01-09) were assessed across 20 weeks (Table 2.2).

To test the effects of hibernaculum removal during budworm diapause on motility (as a proxy to survival) during simulated fall and winter, one experimental group was removed from cheesecloth prior to the start of the fall and winter simulation, while the other remained in cheesecloth and, consequently, their hibernacula for part of the fall and winter simulation. At timepoints 01-09, the motility was assessed for one replicate of budworm that had previously been removed from their hibernacula, and one replicate of budworm that were removed from their cheesecloth patch at that timepoint. That is, except for timepoint 06, which only included a cheesecloth replicate. Each timepoint included one replicate per experimental group consisting of 50 larvae (budworm removed from hibernaculum prior to temperature incubation) or more than 50 larvae (budworm in cheesecloth patches until their timepoint).

Experimental Design #2:

Effect of Hibernaculum Removal Before & During Winter or Post-Winter Dispersal

At the time of motility assessments, I further separated select timepoints (01-09) into new tubes for a post-winter dispersal experiment. Budworm originally in cheesecloth were either maintained in cheesecloth throughout the experiment or removed from the cheesecloth at the time of motility assessment. I compared these two groups to better understand how hibernaculum removal at different times affects the budworm's dispersal ability after diapause. The budworm that remained in cheesecloth throughout the fall and overwintering simulation in addition to the dispersal experiment served as a control group, whereas the group which had been removed from cheesecloth at the beginning of the experiment served as a comparison to the transcriptomic time fall series (Fig. 2.3). For budworm that were checked for motility at 2 °C (timepoints 04-09), both experimental groups (with and without hibernaculum) were followed up on in the dispersal experiment. Note that timepoint 06 only included the two cheesecloth treatments (always in cheesecloth or removed later) and not a comparison without cheesecloth.

To measure dispersal, each budworm replicate was placed in a Petri dish representing a dispersal arena for 5 weeks after overwintering, starting March 12 and ending April 16, 2025. During this period, budworm remained in a MIR-154 incubator at

20 °C and 16:8 h Light:Dark. Dispersal was measured as the larvae's ability to leave their point of origin, either a tube or cheesecloth patch depending on experimental treatment, and venture into the arena. I checked the dispersal arenas for activity three times a week, before tallying their final dispersal at the end of the experiment. Considering that second-instar larvae must be able to move and feed to continue their life cycle post-winter, dispersal served as an ecologically relevant indicator of survival.

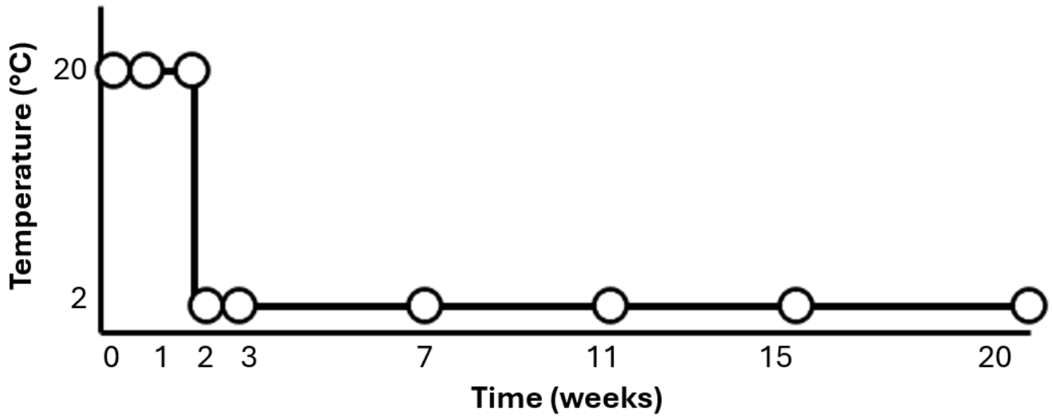

Figure 2.5. Temperature exposures used to measure the effect of budworm hibernaculum on the motility of larvae during fall/winter and post-winter dispersal. Budworm at 2 °C were used for a dispersal experiment after 20 weeks of incubation, while budworm at 20 °C were only included if originally in cheesecloth. The 7-week timepoint only included a replicate with intact hibernacula, but not a replicate without hibernacula. All were assessed for motility at each timepoint described in Table 2.2. The simulation followed a 17-day warm fall (20 °C and 16:8 h Light:Dark) followed by an 18-week overwintering period (2 °C and total darkness) and concluding with a 2-day post-winter warming (20 °C and 16:8 h Light:Dark)

Table 2.2. Incubation durations used in experiments examining the effect of budworm hibernaculum on motility during fall/winter and dispersal after winter. Budworm that remained in their hibernacula or were removed from hibernacula were exposed to a 17-day warm fall (20 °C and 16:8 h Light:Dark) followed by an 18-week overwintering period (2 °C and 0:24 h Light:Dark) and concluding with a 2-day post-winter warming (20 °C and 16:8 h Light:Dark).

Time-point	**Time in fall conditions**	**Time in winter conditions**	**Time in post-winter conditions**	**Total incubation time**
01	2 days	N/A	N/A	2 days
02	1 week	N/A	N/A	1 week
03	2 weeks	N/A	N/A	2 weeks
04	2 weeks 3 days	2 days	N/A	2 weeks 5 days
05	2 weeks 3 days	1 week	N/A	3 weeks 3 days
06	2 weeks 3 days	5 weeks	N/A	7 weeks 3 days
07	2 weeks 3 days	7 weeks	N/A	9 weeks 3 days
08	2 weeks 3 days	10 weeks	N/A	12 weeks 3 days
09	2 weeks 3 days	18 weeks	N/A	20 weeks 3 days

Experimental Set-Up

Budworm without hibernaculum and with hibernaculum destined for time-specific or no removal were moved into tubes on subsequent days. On the same day as removal from rearing conditions within the hatching pans, budworm were removed from hibernacula and transferred to 1.5 mL microcentrifuge tubes, following the same procedure as the fall time series. Due to personnel and time constraints, budworm in cheesecloth patches were moved into tubes on the following day. All larvae were haphazardly assigned an experimental timepoint and moved into a MIR-154 incubator pre-set to 20 °C and 16:8 h Light:Dark at the same time. After one day in the 20 °C incubator, I cut up patches of cheesecloth (ca. 3.0 × 1.8 cm) and assigned these to one of two hibernaculum groups; budworm always in hibernaculum or removed from hibernaculum at different times during the experiment. Each patch contained a minimum of 50 larvae (average of ca. 85), equivalent to a replicate for budworm removed from hibernaculum. I gently rolled up each cheesecloth patch and placed them inside screwcap tubes set up as described previously, which were then transferred into a 20 °C 16:8 h Light:Dark incubator on the same day.

During motility assessments at each timepoint (Fig. 2.5), I assessed motility from one tube of budworm with early hibernaculum removal, and one tube of budworm containing cheesecloth, i.e., budworm with intact hibernacula. At the time of a temperature change (i.e., fall simulation → winter simulation → post-winter warming), I immediately transferred budworm to an incubator pre-set to the new temperature (Table 2.2). Motility was assessed at room temperature as described in the "Motility & Survival Assessment" section. Budworm categorized as motile were moved back to their original screwcap tube, while I transferred immobile budworm to a new 1.5 mL microcentrifuge snap-cap tube, also perforated and covered with a piece of paper towel. After 24 hours, I returned the motile and immobile tube to the incubator, where they resumed and completed the simulation (Fig. 2.5) for later use in assessing dispersal post-winter.

The morning after moving budworm from the winter simulation to post-winter warming, they were relocated to a lab bench for transfer to dispersal arenas, which would be used to test their ability to disperse. I transferred each combination of timepoint (04-09) × hibernaculum (early removal/time-specific removal/no removal) × motility (motile/immobile) to an individual arena. One plastic petri dish or its cover (VWR International, Mississauga, Ontario, Canada) enclosed with Parafilm represented one dispersal arena. The budworm's point of origin, either a tube or cheesecloth patch, was placed in one half of the arena. Tubes containing budworm without cheesecloth were secured to the bottom of the arena using masking tape, while cheesecloth patches were removed from the tubes they were incubated in and left lying in the arena. Cardboard covering and masking tape shaded the half of the arena containing the point of origin. The other half remained unshaded and had light access during the 16:8 h Light:Dark cycle. Light access to half of the arena provided an attractive signal to encourage budworm dispersal, conceptually similar to the hatching pan set-up (Fig. 2.2B).

I randomly assigned each dispersal arena a petri dish (height of 1.4 cm) or petri dish cover (height of 0.9 cm) to one of three incubator shelves. The three shelves were 18 cm, 29.5 cm, or 37.5 cm away from the incubator's light source. Furthermore, escaped larvae prompted a transfer for cheesecloth patches to new arenas after 2 weeks. I transferred cheesecloth patches from plastic petri dishes to PYREX glass dishes (height of 1.6 cm; Corning, NY, USA), as Parafilm clung more securely to the glass surface. Escaped budworm were accounted for using photos of cheesecloth patches taken at the start of the experiment.

Chapter 3: Results

Fall Time Series Transcriptome and Motility

Transcriptome Summary

Génome Québec assembled 71 *C. fumiferana* RNA libraries from 15 treatment groups (control and warm/cool fall × time), of which two libraries were excluded due to RIN scores < 2 during quality control in addition to high overrepresentation of rRNA sequences in FastQC (Andrews, 2010). After excluding the two replicates in question from timepoints 01 (warm fall) and 03 (cool fall), the 69 remaining libraries passed quality control in FastQC. Following trimming in Trimmomatic (Bolger et al., 2014), 86.19% to 89.50% of RNA sequencing reads from each replicate aligned with the NCBI reference genome in HISAT2 (Kim et al., 2019).

Spruce Budworm in an Early Warm Fall or Late Cool Fall Overlap in Gene Expression

In a principal component analysis (PCA), spruce budworm gene expression overlapped between ten weeks of cool fall and the first two weeks of warm fall (Fig. 3.1). After 4 weeks in a warm fall, budworm gene expression differed from the cool and early warm fall groups and continued to change over time along principal component 1 (PC1), which explained 55% of variance in gene expression data. Meanwhile, all cool fall groups and the first two weeks of warm fall aligned along principal component 2, which explained 11% of the variance. Of the 500 most influential genes in the PCA, 293 genes contributed above the expected average contribution to PC1 and 105 genes to PC2 (Fig. 3.2).

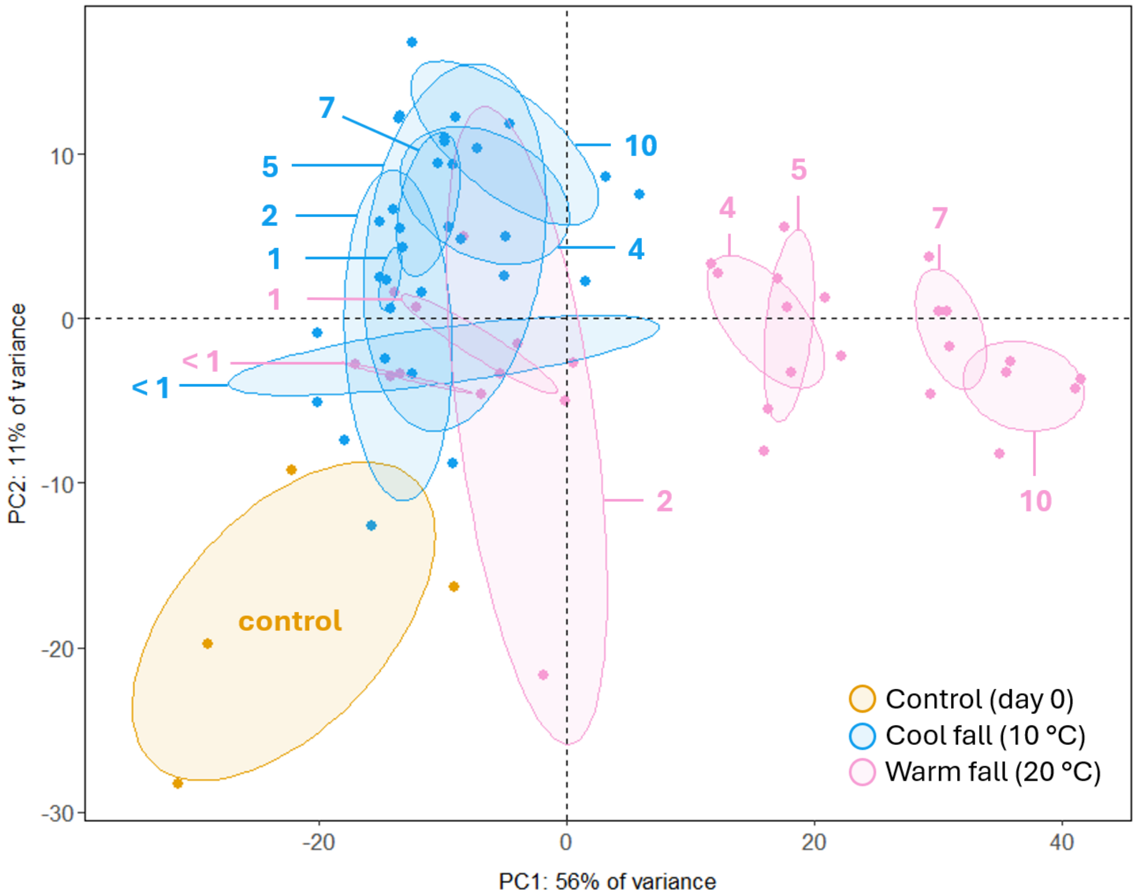

Figure 3.1. Variation in gene expression drives separation along principal components 1 (PC1) and 2 (PC2) of *C. fumiferana* larvae during 10 weeks of warm (20 °C; pink) or cool (10 °C; blue) fall conditions. Each dot represents one biological replicate of 50 pooled larvae. Orange indicates the control (day 0) treatment. Circles around each treatment group indicate 95% confidence intervals. Lines point to the number of weeks per treatment group.

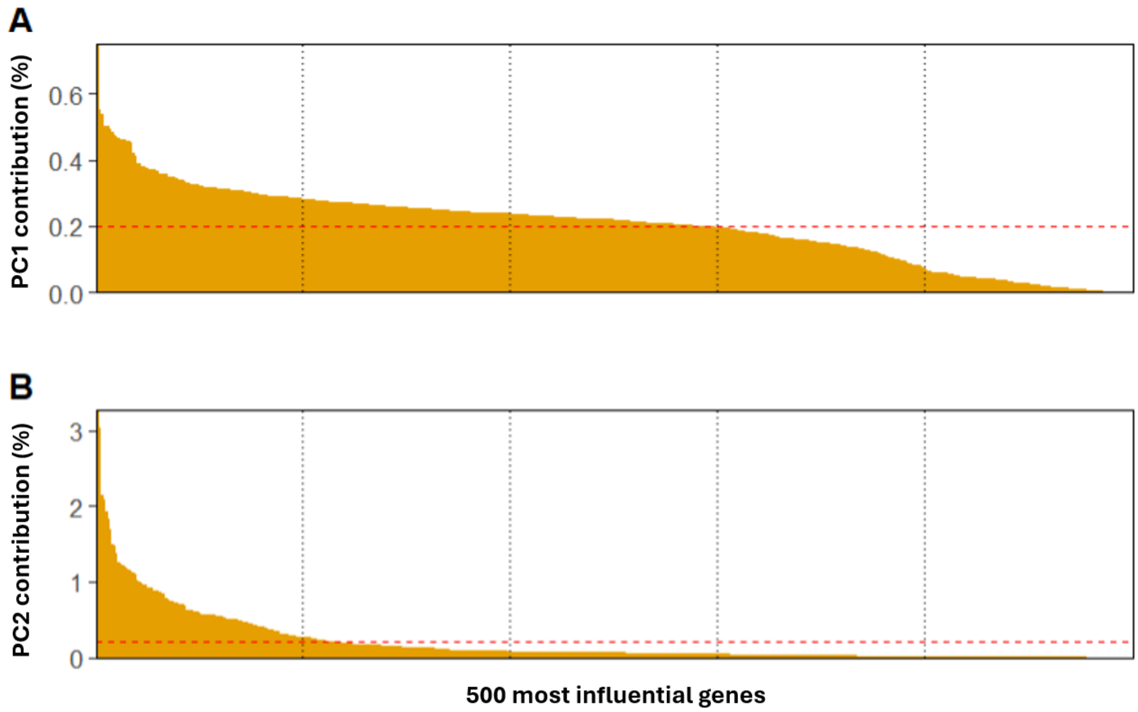

Figure 3.2. Contribution (%) by genes to principal component (PC) comparisons of *C. fumiferana* during 10 weeks of warm (20 °C) or cool (10 °C) fall conditions (Fig. 3.1). **A.** Gene contribution (%) to PC1. **B.** Gene contribution (%) to PC2. A red dashed line indicates the expected average contribution (%) of the 500 most influential genes. Each orange bar represents one gene.

Genes Cluster Into Expression Profiles Based on Response to Temperature and Time

In maSigPro, significantly differentially expressed genes clustered into eight distinct expression profiles (Fig. 3.3). I assigned five potential patterns to the clusters (Fig. 3.3): warm-responsive (A), early diapause increase (B), early diapause peak (C-D), diapause delayed decrease (E-F), and early diapause decrease (G-H).

In cluster A, gene expression increased steadily in the warm fall and remained low in the cool fall (Fig. 3.3A). GO terms related to transcription and asymmetric cell division were enriched in this cluster (Table 3.1).

Warm fall gene expression similarly increased in cluster B, but with more overlap in the first two weeks of warm and cool falls, and a gradual increase in the cool fall (Fig. 3.3B). This cluster was enriched for only two GO terms: “regulation of transcription by RNA polymerase II” and “ubiquitin-dependent protein catabolic process” (Table 3.1).

Clusters C and D displayed a “peak” pattern most closely aligned to one of my predicted gene expression patterns (Figs. 1.2 & 3.3C-D). In these clusters, gene expression increased for two weeks in a warm fall and seven weeks in the cool fall, before it decreased (Fig. 3.3C-D). Both clusters were enriched for GO terms related to general transcription and translation processes, as well as the Notch signalling pathway, which regulates cell development (Table 3.1).

Remaining cluster profiles showed decreases in overall gene expression with some variation (Fig. 3.3E-H). Clusters E and F showed stable expression levels during the first two weeks of a warm fall and first seven weeks of the cool fall, followed by a decrease in gene expression (Fig. 3.3E-F). This trend aligns with the inverse of one of my predicted gene expression patterns (Fig. 1.2). GO terms related to DNA processes, nitrogen metabolism, the tricarboxylic acid cycle, and cell transport and signalling were enriched in these two clusters (Table 3.1).

Lastly, clusters G and H displayed a decrease in gene expression in both warm and cool falls, with almost identical trajectories in cool and warm falls for cluster G, and higher expression values in cool than warm fall conditions for cluster H (Fig. 3.3G-H). These clusters were enriched for GO terms for protein processes, inositol catabolism, and fatty acid biosynthesis (Table 3.1).

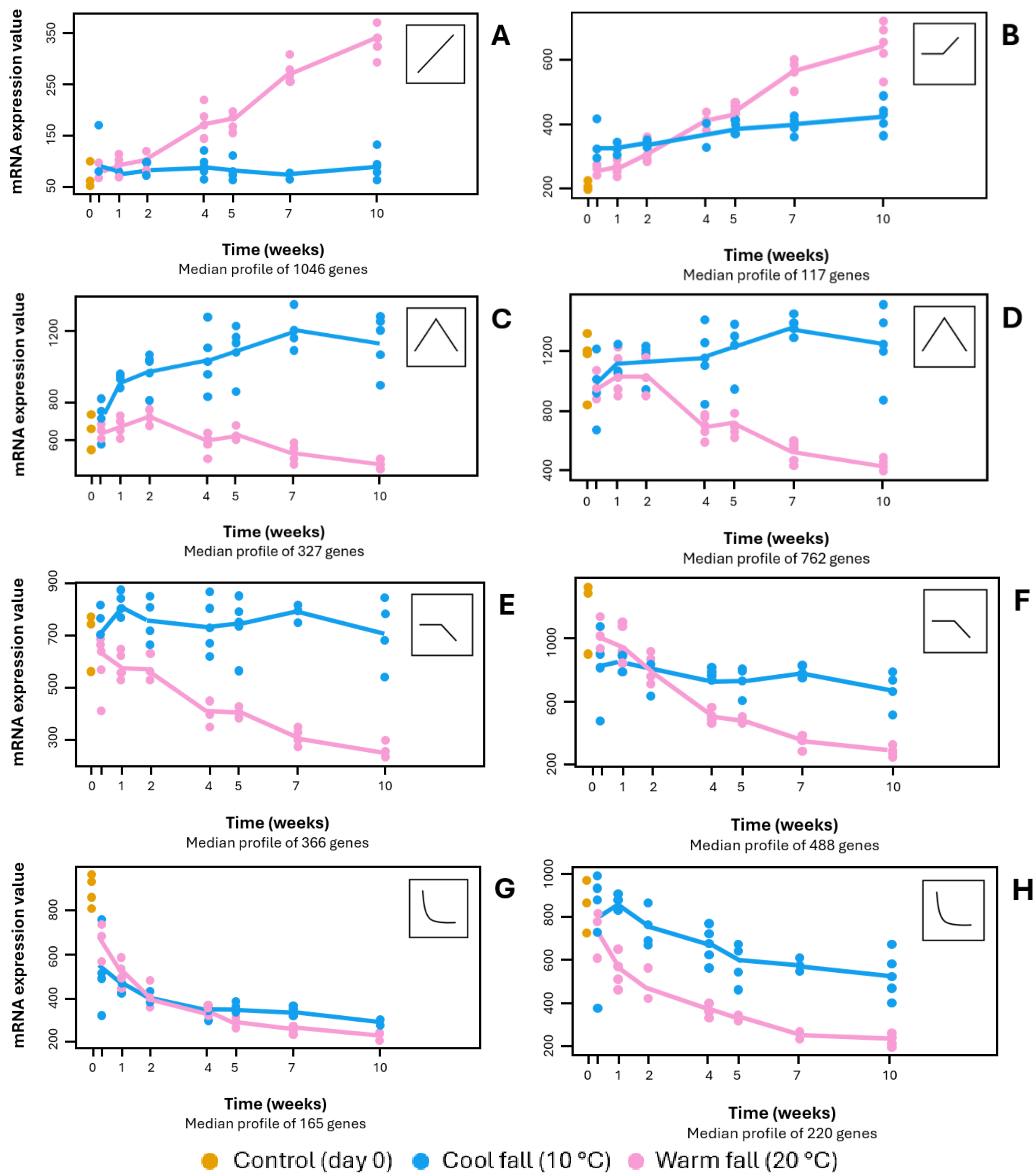

Figure 3.3. Gene profile clusters (**A-H**) from maSigPro show changes in mRNA expression values for *C. fumiferana* larvae during 10 weeks of warm (20 °C; pink) or cool (10 °C; blue) fall conditions. Orange indicates the control (day 0) treatment. Gene expression determined from 3-5 biological replicates of 50 pooled larvae per fall treatment × time combination. Boxed icon in the top right corner represents a simplified shape of the predicted or inferred trend.

Table 3.1. Enriched GO terms (biological processes) of maSigPro (mSP) warm and cool fall clusters (Fig. 3.2). Predicted gene profiles would occur earlier in a warm fall, and later in a cool fall (except for clusters G and H). Significant:Annotated (S:A) ratios indicate the number of genes that were significantly enriched compared to the number of genes representing that GO term in the genome. When the significant number of genes exceeds the expected number of genes, this results in a P-value < 0.05, as determined by the Fisher's exact test in topGO.

Predicted Gene Profile	mSP Cluster ID	GO ID	GO Term	S:A	Expected	P-value
Warm-responsive	A	GO:0006355	regulation of DNA-templated transcription	32:179	16.71	0.001
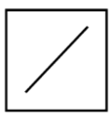		GO:0008356	asymmetric cell division	2:2	0.19	0.009
		GO:0032784	regulation of DNA-templated transcription elongation	2:2	0.19	0.009
		GO:0006207	'de novo' pyrimidine nucleobase biosynthetic process	3:7	0.65	0.021
		GO:0006821	chloride transport	2:3	0.28	0.024
		GO:0006378	mRNA polyadenylation	2:3	0.28	0.024
		GO:0006357	regulation of transcription by RNA polymerase II	7:34	3.17	0.034
		GO:0070897	transcription preinitiation complex assembly	3:5	0.47	0.046
Early diapause increase	B	GO:0006357	regulation of transcription by RNA polymerase II	4:34	0.55	0.002
		GO:0006511	ubiquitin-dependent protein catabolic process	3:48	0.77	0.040

Table 3.1. continued.

Predicted Gene Profile	mSP Cluster ID	GO ID	GO Term	S:A	Expected	P-value
Early diapause peak	C	GO:0006364	rRNA processing	4:17	0.51	0.009
		GO:0030163	protein catabolic process	5:57	1.71	0.021
		GO:0006412	translation	6:84	2.52	0.034
		GO:0006633	fatty acid biosynthetic process	2:10	0.3	0.034
	D	GO:0006412	translation	26 :84	5.42	<0.001
		GO:0006465	signal peptide processing	3:4	0.26	0.001
		GO:0006366	transcription by RNA polymerase II	5:45	2.91	0.005
		GO:0006364	rRNA processing	7:17	1.1	0.007
		GO:0000398	mRNA splicing, via spliceosome	5:22	1.42	0.011
		GO:0043248	proteasome assembly	2:3	0.19	0.012
		GO:0006614	SRP-dependent cotranslational protein targeting to membrane	2:4	0.26	0.023
		GO:0007219	Notch signalling pathway	2:5	0.32	0.036
		GO:0015986	proton motive force-driven ATP synthesis	2:5	0.32	0.036
		GO:0006396	RNA processing	22: 108	6.97	0.038
		GO:1902600	proton transmembrane transport	3:12	0.77	0.038

Table 3.1. continued.

Predicted Gene Profile	**mSP Cluster ID**	**GO ID**	**GO Term**	**S:A**	**Expected**	**P-value**
Diapause delayed decrease 	E	GO:0006099	tricarboxylic acid cycle	3:11	0.35	0.004
		GO:0006302	double-strand break repair	3:7	0.22	0.009
		GO:0016192	vesicle-mediated transport	8:71	2.25	0.027
		GO:0006888	endoplasmic reticulum to Golgi vesicle-mediated transport	2:10	0.32	0.038
	F	GO:0042274	ribosomal small subunit biogenesis	2:4	0.1	0.004
		GO:0032508	DNA duplex unwinding	2:7	0.18	0.012
		GO:0006807	nitrogen compound metabolic process	33:1149	28.82	0.013
		GO:0006270	DNA replication initiation	2:8	0.2	0.016
		GO:0007264	small GTPase mediated signal transduction	2:14	0.35	0.046
		GO:0071897	DNA biosynthetic process	2:3	0.08	0.049
Early diapause decrease 	G	GO:0019310	inositol catabolic process	2:3	0.02	<0.001
		GO:0006457	protein folding	3:21	0.24	0.002
	H	GO:0006633	fatty acid biosynthetic process	2:10	0.22	0.019
		GO:0006511	ubiquitin-dependent protein catabolic process	4:48	1.05	0.038

Warm-Responsive Genes Influence PC1

While genes from all clusters were present in PC1, 62.9% of genes in PC1 were associated with cluster A, suggesting most genes associated with PC1 increased in expression during the warm fall (Figs. 3.1 & 3.3A). Thus, the GO term enrichments identified with cluster A likely represent processes that are enriched in PC1 (Table 3.1). The top 10 contributing genes in PC1 consisted of various enzymes, such as lipase and kinases, in addition to genes related to neural activity (*Shark*, *zig-3*, and cyclic AMP-responsive element-binding protein), cellular processes (*dSOR1* and F-box protein), and hormone signalling (*HR38*; Table 3.2). Other genes of interest that contributed to PC1 included insulin-like growth factor 2, glucose dehydrogenases, and glycerol kinases. Immune system-related genes also contributed, expressed through some immunoglobins, interferons, and antigens. Genes related to asymmetric cell division, like lethal (2) giant larvae protein, were also present. Lastly, 66 of 283 genes above the expected average contribution in PC2 were of unknown function.

Table 3.2. Top 10 genes which contribute (%) to Principal Component 1 (PC1) during a warm or cool fall time series in C. fumiferana (Fig. 3.1). If the protein function for the reference genome's Gene ID (number following MSG28_ in annotation) was unknown, a BLAST search was performed through NCBI. PC loadings (1 & 2) and available maSigPro Cluster IDs (Fig. 3.3) provided per Gene ID.

Gene ID	*C. fumiferana* Annotation	BLAST Result [Accession]	PC1 (%)	PC Loadings		Cluster ID
				PC1	PC2	
006414	Lipase member I	-	0.749	-0.087	-0.052	H
010719	Unknown	Uncharacterized	0.553	-0.074	-0.042	F
006242	Unknown	89% similar to A-kinase anchor protein 200-like [XP_061704029.1]	0.537	0.073	-0.014	A
011153	Tyrosine-protein kinase Shark	-	0.504	0.071	-0.028	A
002277	Probable nuclear hormone receptor HR38 (Fragment)	-	0.503	0.071	-0.031	A
015809	Zwei Ig domain protein zig-3	-	0.501	0.071	-0.030	A
012792	F-box/LRR-repeat protein 14	-	0.494	0.070	-0.023	A
003460	Cyclic AMP-responsive element-binding protein 1	-	0.483	0.069	-0.002	A
012396	Dual specificity mitogen-activated protein kinase dSOR1	-	0.476	0.069	-0.023	A
004673	Unknown	Uncharacterized	0.470	0.069	-0.005	A

Cuticle and Silk Production Genes Influence PC2

Out of the top 10 contributing genes in PC2, most genes encoded for unknown proteins which had some similarities to either cuticle- or seroin-related genes, as determined by NCBI's BLAST search (Table 3.3). In insects, the cuticle provides exterior structural support while seroin is used in silk production (Qi & Liu, 2025; Dong et al., 2023). PC2 contained 30 fully characterized cuticular proteins with an above average contribution to variation, whereas PC1 only included 7. While most maSigPro clusters, except for D and H, appeared in PC2, cluster C was most abundant and represented 15.38% of PC2 (Figs. 3.1 & 3.3). In the overlap between PC2 and cluster C, seroin proteins (Table 3.4), fatty acid metabolism (Table 3.5), and *Cf*AFPs (Table 3.6) were all expressed. Lastly, 62 of 104 genes above the expected average contribution in PC2 were of unknown function.

Gene Expression of Diapause-Related Processes

Tables 3.4-6 include genes I predicted to be relevant to early budworm diapause (Table 1.1) that appeared in PC2 or gene clusters (Figs. 3.1 and 3.3). Namely, in the "early diapause peak" cluster C, a diapause hormone homologue (Pyrokinin-1 receptor) and the insulin-related Bombyxin hormone were both present (Table 3.4). Cluster D, which shares a similar profile to C, also included Wnt signalling, circadian rhythm, *PCNA*, and antioxidant genes (Tables 3.4 and 3.6). However, contradictory to my initial predictions (Table 1.1), some glycerol-, insulin-, and juvenile hormone-related genes appeared in other clusters, such as "warm-responsive" cluster A (Tables 3.4-6).

The gene expression of other possibly diapause-related proteins, *Cf*DAP1 and *Cf*HSPs, did not appear in PC2 or gene clusters and were investigated separately. The gene expression of *Cf*DAP1 was highest on day 0 and remained present throughout both warm and cool falls (Fig. 3.4F). In a linear regression model (P < 0.001), *Cf*DAP1 expression was significantly affected by fall temperature (P = 0.003) but not time in fall (P = 0.011) or the interaction between temperature and time (P = 0.626). 13 *Cf*HSPs were significantly differentially expressed based on linear regression models (Table 3.7). *Cf*HSP21.3, *Cf*HSP24.3, *Cf*HSP19.2, *Cf*HSP19.7, and *Cf*HSP19.6 had high gene expression (Fig. 3.7A-E), whereas the other 8 *Cf*HSPs had read counts below 30. *Cf*HSP21.3 and *Cf*HSP24.3 were the only HSPs that primarily increased their gene expression during the cool fall while decreasing in a warm fall (Fig. 3.4A & B). *Cf*HSPs19.2, *Cf*HSP19.7, and *Cf*HSP19.6 had increased expression in the warm fall and remained low in the cool fall (Fig. 3.4C-E).

Table 3.3. Top 10 genes which contribute (%) to Principal Component 2 (PC2) during a warm or cool fall time series in *C. fumiferana* (Fig. 3.1). If the protein function for the reference genome's Gene ID (number following MSG28_ in annotation) was unknown, a BLAST search was performed through NCBI. PC loadings (1 & 2) and available maSigPro Cluster IDs (Fig. 3.3) provided per Gene ID.

Gene ID	***C. fumiferana* Annotation**	**BLAST Result [Accession]**	**PC2 (%)**	**PC Loadings**		**Cluster ID**
				PC1	**PC2**	
010810	Protein of unknown function	48% similar to seroin-like isoform X1 [XP_047984770.1]	3.281	-0.013	0.181	C
007628	Cuticle protein 8	-	3.031	-0.051	-0.174	-
010102	Protein of unknown function	tweedleT (*C. fumiferana*) [XP_073956664.1]	2.147	-0.021	-0.147	-
005204	Protein of unknown function	78% similar to cuticle protein LPCP-23-like [XP_063363722.1]	1.921	-0.049	-0.139	-
002598	Flexible cuticle protein 12	-	1.837	-0.042	-0.136	-
009647	Protein of unknown function	66% similar to cuticle protein 16.5-like [XP_063362997.1]	1.503	-0.040	-0.123	-
009649	Protein of unknown function	74% similar to cuticle protein 64-like [XP_063381344.1]	1.472	-0.036	-0.121	-
007845	Protein of unknown function	82% similar to larval/pupal cuticle protein H1C-like [XP_045449371.1]	1.384	-0.055	-0.118	-
002625	Neurofilament heavy polypeptide	-	1.258	-0.038	-0.112	-
015137	Pupal cuticle protein PCP52	-	1.246	-0.040	-0.112	-

Table 3.4. Select transcripts with potential implications for arrested development from Principal Component 2 (PC2; Fig. 3.1) or maSigPro clusters (A-H; Fig. 3.3) during a fall time series in diapausing *C. fumiferana*. If the protein function for the reference genome's Gene ID was unknown, a BLAST search for fully characterized protein sequences with the highest percentage identity match was performed through NCBI. InterPro signature included as relevant. Contributions (%) to PC2 and PC loadings given as relevant.

Diapause-Associated Category	**Gene ID**	***C. fumiferana* Annotation, {InterPro}, or BLAST [Accession]**	**PC2 (%)**	**PC Loadings**		**Cluster ID**
				PC1	**PC2**	
Silk Production	010810	48% similar to seroin-like isoform X1 [XP_047984770.1]	3.281	-0.013	0.181	C
	013877	Similar to Seroin (*Galleria mellonella*)	0.563	-0.036	0.075	C
	013876	Similar to Seroin (*Galleria mellonella*)	0.481	-0.027	0.069	-
	005207	68% similar to fibroin heavy chain-like [XP_063535600.1]	0.497	-0.046	-0.070	-
Larval/Pupal Development	009459	Similar to SP1: Sex-specific storage-protein 1 (*Bombyx mori*)	0.693	-0.021	-0.083	-
	011415	Similar to VG: Vitellogenin (*Bombyx mori*)	0.512	-0.008	-0.072	-
	013180	Similar to AJSP-1: Acidic juvenile hormone-suppressible protein 1 (*Trichoplusia ni*)	0.314	-0.010	-0.056	-

Table 3.4. continued.

Diapause-Associated Category	**Gene ID**	***C. fumiferana* Annotation, {InterPro}, or BLAST [Accession]**	**PC2 (%)**	**PC Loadings**		**Cluster ID**
				PC1	**PC2**	
Larval/Pupal Development	000567, 000622, 001682, 002957, 009670, 009799; 008812, 009910; 002964; 012873	{Juvenile hormone binding proteins}; Juvenile hormone (JH) esterases; JH acid O-methyltransferase; JH epoxide hydrolase	-	-	-	F
	006463	Similar to Tcjhe: Juvenile hormone esterase (*Tribolium castaneum*)	-	-	-	D
	012872	Similar to JHEH: Juvenile hormone epoxide hydrolase (*Bombyx mori*)	-	-	-	A
	005294, 006648; 010946, 000447	Juvenile hormone (JH) esterases; {JH binding proteins}	-	-	-	G
	003405	Similar to Eip75B: Ecdysone-induced protein 75B, isoform A (*Drosophila melanogaster*)	-	-	-	H
	004919	Similar to SBXA3: Bombyxin A-3 homolog (*Samia cynthia*)	-	-	-	C

Table 3.4. continued.

Diapause-Associated Category	**Gene ID**	***C. fumiferana* Annotation, {InterPro}, or BLAST [Accession]**	**PC2 (%)**	**PC Loadings**		**Cluster ID**
				PC1	**PC2**	
Diapause Hormone	006258	Similar to PK1-R: Pyrokinin-1 receptor (*Drosophila melanogaster*)	0.919	0.024	0.096	C
Photoreceptor	005203	{*Drosophila* Retinin like protein}	0.272	-0.052	-0.062	G
Circadian Rhythm	002193	Similar to tim: Protein timeless (*Drosophila melanogaster*)	-	-	-	D
	000574	Similar to dyw: Circadian clock-controlled protein daywake (*Drosophila melanogaster*)	-	-	-	D
DNA Synthesis	007401	Similar to PCNA: Proliferating cell nuclear antigen (*Bombyx mori*)	-	-	-	D
Wnt Signalling	002054	Similar to WNT-1: Protein Wnt-1 (*Bombyx mori*)	-	-	-	D
	003056	Similar to TMEM181: Transmembrane protein 181 (*Homo sapiens*)	-	-	-	F

Table 3.5. Select transcripts with potential implications for metabolic restructuring from Principal Component 2 (PC2; Fig. 3.1) or maSigPro clusters (A-H; Fig. 3.3) during a fall time series in diapausing *C. fumiferana*. If the protein function for the reference genome's Gene ID was unknown, a BLAST search for fully characterized protein sequences with the highest percentage identity match was performed through NCBI. InterPro signature included as relevant. Contributions (%) to PC2 and PC loadings given as relevant.

Diapause-Associated Category	**Gene ID**	***C. fumiferana* Annotation, {InterPro}, or BLAST [Accession]**	**PC2 (%)**	**PC Loadings**		**Cluster ID**
				PC1	**PC2**	
Lipid Metabolism & Transport	011618	Similar to Apolipophorins (*Manduca sexta*)	0.288	0.022	-0.054	-
	012173	Similar to Lip1: Lipase 1 (*Drosophila melanogaster*)	0.211	-0.024	-0.046	-
Fatty Acid Membrane Remodeling	006259	Similar to Acyl-CoA Delta-9 desaturase (*Acheta domesticus*)	0.726	0.020	0.085	C
	006260	Similar to Acyl-CoA Delta-9 desaturase (*Acheta domesticus*)	0.315	0.056	0.072	A
	008137	Similar to Acyl-CoA Delta-9 desaturase (*Acheta domesticus*)	0.600	0.013	-0.077	-
	014966	Similar to Acyl-CoA Delta(11) desaturase (*Choristoneura rosaceana*)	0.227	-0.048	-0.048	F

Table 3.5. continued.

Diapause-Associated Category	**Gene ID**	***C. fumiferana* Annotation, {InterPro}, or BLAST [Accession]**	**PC2 (%)**	**PC Loadings**		**Cluster ID**
				PC1	**PC2**	
Insulin Signalling	000979	Similar to IGF2BP1: Insulin-like growth factor 2 mRNA-binding protein 1 (*Gallus gallus*)	-	-	-	A
	014409	Similar to Ide: Insulin-degrading enzyme (*Drosophila melanogaster*)	-	-	-	A
	010658	Similar to Igfals: Insulin-like growth factor-binding protein complex acid labile subunit (*Mus musculus*)	-	-	-	F
	001059	Similar to Insulin-related peptide 2 (*Agrotis ipsilon*)	-	-	-	G
	002569	Similar to igf1r: Insulin-like growth factor 1 receptor (*Xenopus laevis*)	-	-	-	H
Glycogen Metabolism	010796	Similar to GYG1: Glycogenin-1 (*Homo sapiens*)	-	-	-	G

Table 3.6. Select transcripts with potential implications for stress tolerance from Principal Component 2 (PC2; Fig. 3.1) or maSigPro clusters (A-H; Fig. 3.3) during a fall time series in diapausing *C. fumiferana*. If the protein function for the reference genome's Gene ID was unknown, a BLAST search for fully characterized protein sequences with the highest percentage identity match was performed through NCBI. InterPro signature included as relevant. Contributions (%) to PC2 and PC loadings given as relevant.

Diapause-Associated Category	**Gene ID**	***C. fumiferana* Annotation, {InterPro}, or BLAST [Accession]**	**PC2 (%)**	**PC Loadings**		**Cluster ID**
				PC1	**PC2**	
Antifreeze proteins	010645	*Cf*AFP-16	0.845	0.010	0.092	C
	010644	*Cf*AFP-15	0.586	0.014	0.075	C
Immune system	012678	Similar to Attacin-A (*Trichoplusia ni*)	0.263	-0.006	-0.051	B
	015985	{Diapausin family of antimicrobial peptide}	0.240	-0.040	-0.049	F
	014258	Similar to Hyphancin-3E (*Hyphantria cunea*)	0.227	0.012	-0.048	-
Antioxidants	000874	Similar to PRDX6: Peroxiredoxin-6 (*Bos taurus*)	-	-	-	D
	000991	Similar to Cat: Catalase (*Drosophila melanogaster*)	-	-	-	D
	009975	Similar to Superoxide dismutase [Cu-Zn] (*Bombyx mori*)	-	-	-	D
	013096	Similar to sod-2: Superoxide dismutase [Mn] 1, mitochondrial (*Caenorhabditis elegans*)	-	-	-	D

Table 3.6. continued.

Diapause-Associated Category	Gene ID	*C. fumiferana* Annotation, {InterPro}, or BLAST [Accession]	PC2 (%)	PC Loadings		Cluster ID
				PC1	PC2	
Antioxidants	003456, 003459, 007876, 008846, 013099	Glutathione S-transferases	-	-	-	D
	009981	Similar to Superoxide dismutase [Cu-Zn] (*Bombyx mori*)	-	-	-	E
	001435; 003653	{Superoxide dismutase [Cu-Zn]}; Similar to SOD1: Superoxide dismutase [Cu-Zn] (*Gallus gallus*)	-	-	-	F
	004283, 007960, 008178, 010870, 012269	Glutathione S-transferases	-	-	-	F
Glycerol Metabolism	008748	Similar to gk5: Putative glycerol kinase 5 (*Danio rerio*)	-	-	-	A
	005146	Similar to PGP: Glycerol-3-phosphate phosphatase (*Bos taurus*)	-	-	-	A
	002893	Similar to Gpdh1: Glycerol-3-phosphate dehydrogenase [NAD(+)], cytoplasmic (*Drosophila virilis*)	-	-	-	E

Table 3.7. Effects of a cool (10 °C) or warm (20 °C) fall temperature and time (weeks) on the gene expression of diapause-associated protein 1 (*Cf*DAP1) and 13 *C. fumiferana* heat shock proteins (*Cf*HSPs). Significant *P* values, as determined by linear regression analysis, are bolded. A Bonferroni correction was performed for multiple analyses ($\alpha = 0.050 / 14 = 0.004$).

	***P* value**			
Gene Name	**Linear Regression Model**	**Fall Temperature**	**Time**	**Fall Temperature × Time**
*Cf*HSP20.0	**< 0.001**	0.120	0.964	0.116
*Cf*HSP21.5a	**< 0.001**	0.674	0.068	0.012
*Cf*HSP18.6	**< 0.001**	**< 0.001**	0.204	0.095
*Cf*HSP19.2	**< 0.001**	**< 0.001**	0.482	0.016
*Cf*HSP20.2	**< 0.001**	**< 0.001**	0.709	0.019
*Cf*HSP21.3	**< 0.001**	0.669	0.022	**< 0.001**
*Cf*HSP22.0	**< 0.001**	0.071	0.213	**< 0.001**
*Cf*HSP22.1	**< 0.001**	0.596	0.505	**0.002**
*Cf*HSP23.9	**< 0.001**	0.747	0.640	**< 0.001**
*Cf*HSP19.7	**< 0.001**	**< 0.001**	0.321	**< 0.001**
*Cf*HSP21.5b	**< 0.001**	**< 0.001**	0.885	**< 0.001**
*Cf*HSP24.3	**< 0.001**	**< 0.001**	0.121	**< 0.001**
*Cf*HSP19.6	**< 0.001**	0.033	**< 0.001**	**< 0.001**
*Cf*DAP1	**< 0.001**	**0.003**	0.011	0.626

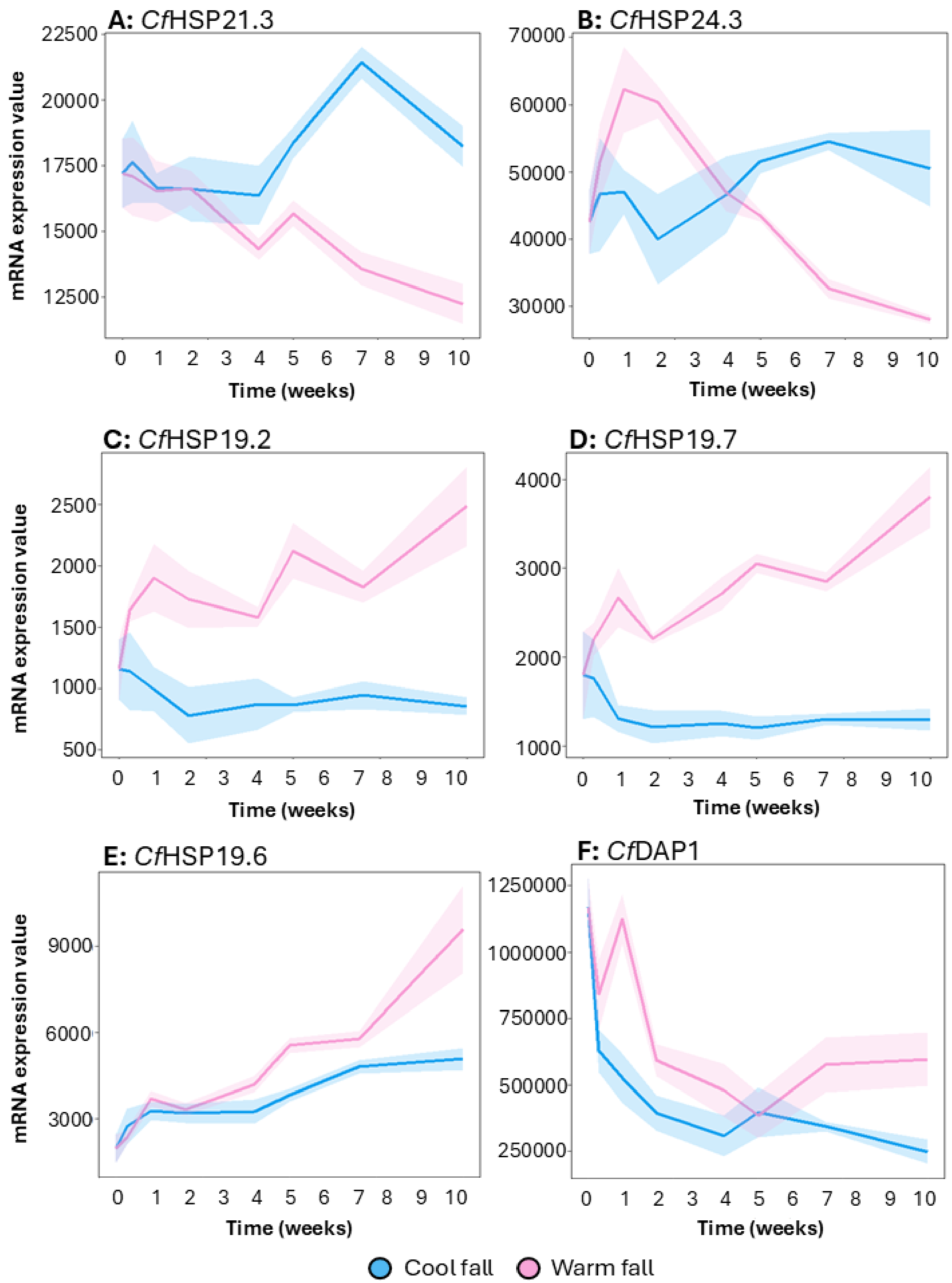

Figure 3.4. Average gene expression of five *C. fumiferana* heat shock proteins (*Cf*HSPs; **A-E**) and diapause associated protein 1 (*Cf*DAP1; **F**) over a 10-week cool (10 °C; blue) or warm (20 °C; pink) fall. Solid lines represent the mean gene expression, and the ribbon represents the standard error of the mean. Gene expression was determined from 3-5 biological replicates of 50 pooled larvae per temperature × timepoint combination. Linear regression statistics are in Table 3.7.

Larval Motility During a Fall Simulation

The proportion of motile budworm decreased during simulated fall conditions at both cool and warm temperatures, and budworm exposed to the warm fall temperature had the lowest motility (Fig. 3.5). At the start of the experiment almost all larvae were motile, and after 10 weeks of simulated fall, approximately half of larvae in the cool fall were still motile, while none were motile in the warm fall (Fig. 3.5). Although motility data is limited for the 1st trial with larvae used for transcriptomics, the proportion of motile of larvae from the second trial appeared representative of what likely happened in the transcriptomics group (Fig. 3.5). As the proportion of motile larvae decreased over time, the proportion of shrunken larvae increased, particularly in the warm fall group (Fig. 3.6). The other immobile categories—immobile L1s, ensnared, and deformed—consisted of smaller portions of larvae and remained relatively consistent over time (Fig. 3.6).

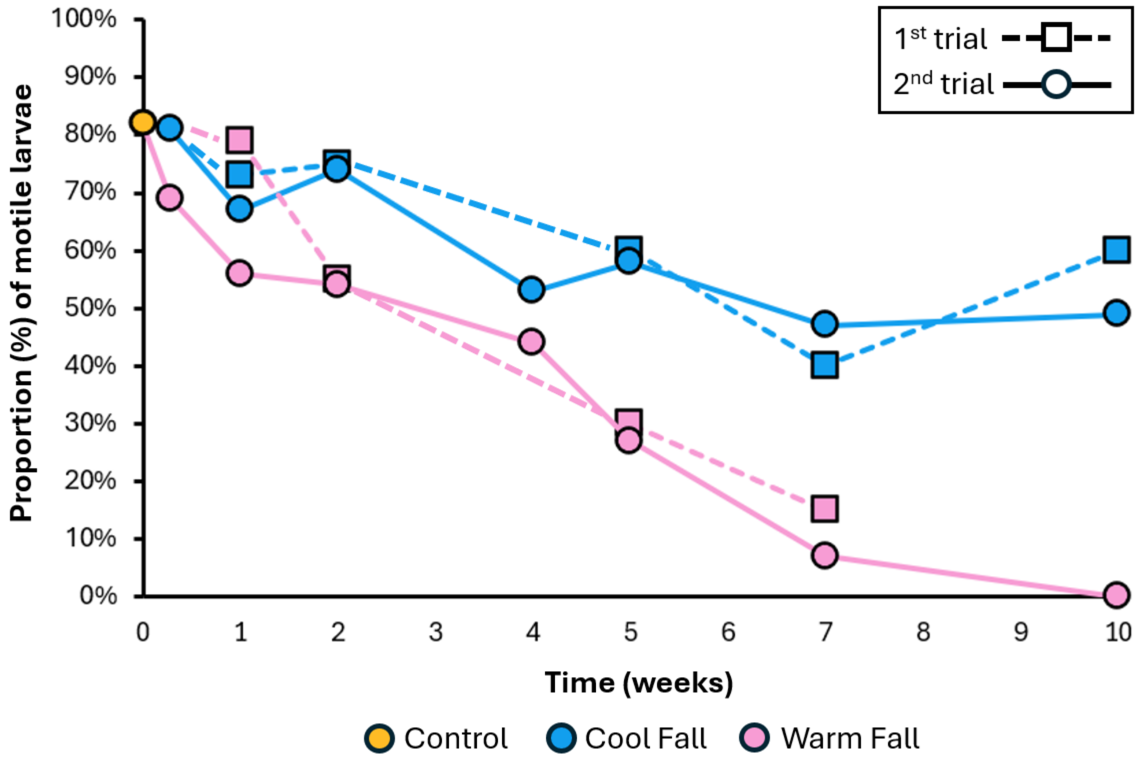

Figure 3.5. Proportion (%) of motile larvae during a 10-week fall (16:8 h Light:Dark) at either a cool (10 °C; blue) or warm (20 °C; pink) temperature. Motile larvae were predominantly second-instar with a small number of first-instar larvae (Fig. 3.6). A control at day 0 is represented by an orange circle. All assessments were conducted at room temperature (ca. 22 °C). Each data point corresponds to the proportion of larvae from a tube totaling 50 budworm. Lines connecting points have been added to guide the eye. Solid lines connect data points from the 2nd trial with motility checks for the full fall time series. Dashed lines connect data points from the 1st trial designated for transcriptomic sequencing for a subset of timepoints

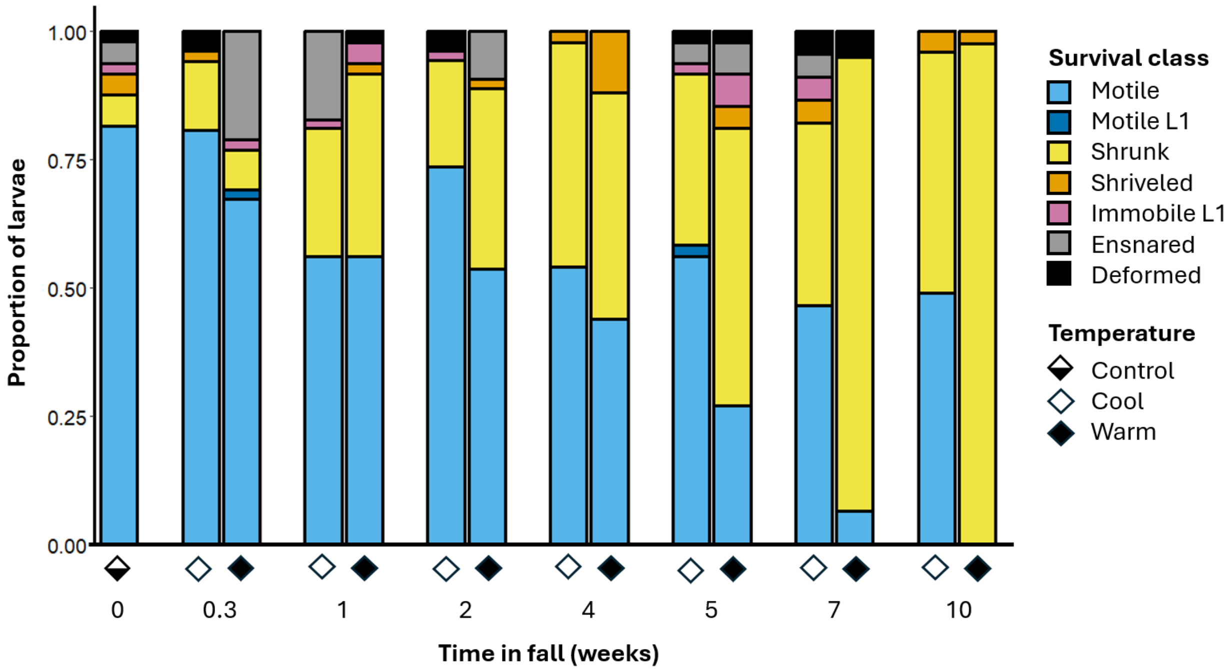

Figure 3.6. Proportion of larvae categorized as one of seven survival classes during simulated fall conditions (16:8 h Light:Dark), at either a cool (10 °C) or warm (20 °C) temperature. Survival classes consisted of second-instar larvae (Fig. 2.4), unless specified as first-instar (L1). ◇ represents budworm exposed to cool fall conditions, and ◆ represents warm fall conditions. ⬙ represents a control at the beginning of the time series. All assessments were conducted at room temperature (ca. 22 °C). Each replicate included 50 larvae.

Effects of Hibernaculum Removal

Larval Motility During an IPQL-like Fall & Winter Simulation

During exposure to IPQL-like overwintering conditions (17 days of warm fall and 18 weeks of winter conditions), budworm in hibernacula fared better than budworm without hibernacula. Budworm in hibernacula had a consistently higher proportion of motile larvae throughout fall and overwintering conditions, while budworm removed from their hibernacula prior to the fall simulation decreased in the proportion of motile larvae over time (Fig. 3.7). Specifically, the proportion of motile larvae without hibernacula decreased steadily between two days and two weeks of fall conditions (Fig. 3.7A). In winter conditions, the proportion of motile larvae without hibernacula continued to decline, to ca. 25% at the end of the simulation (Fig. 3.7B). Meanwhile, the proportion of motile larvae with hibernacula remained at ca. 90% at the end of winter (Fig. 3.7B). As the proportion of motile larvae without hibernacula decreased over time, the proportion of shrunken immobile larvae increased (Fig. 3.8). For budworm in hibernacula, the proportion of motile larvae remained high and immobile classifications consisted largely of L1s that never progressed to L2s (Fig. 3.8).

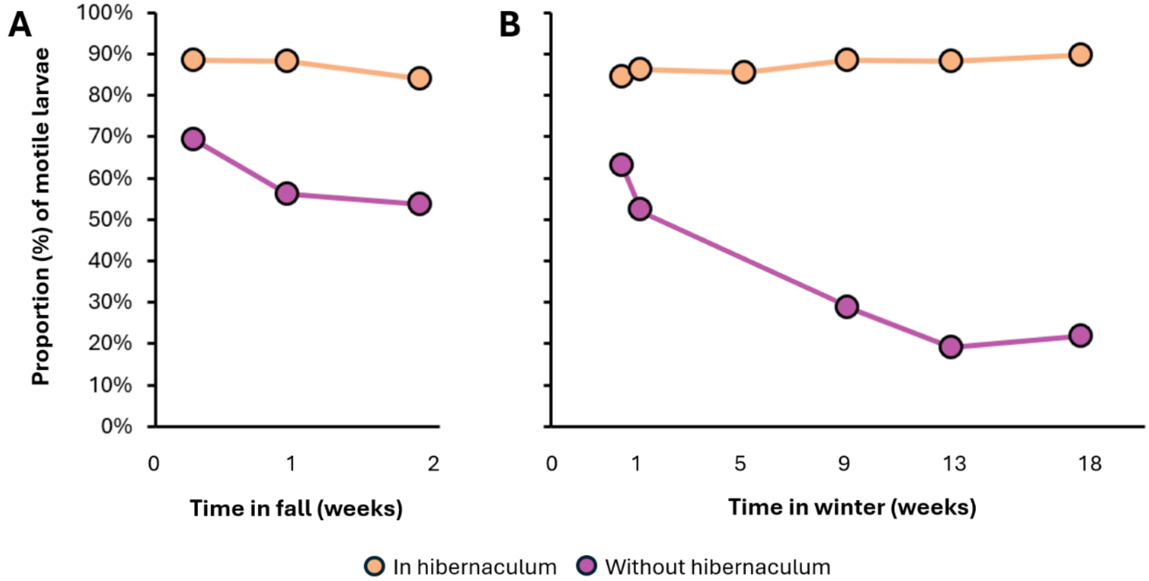

Figure 3.7. Proportion (%) of motile larvae removed from hibernaculum at day 0 (purple) and larvae that remained in hibernaculum until classification of motility (orange). **A)** Larvae in fall conditions (20 °C and 16:8 h Light:Dark). **B)** Larvae in winter conditions (2 °C and total darkness) following 17 days of fall conditions. Lines connecting points have been added to guide the eye. Each replicate for budworm without hibernacula contained 50 larvae while each replicate for budworm in hibernacula contained ≥ 50 larvae.

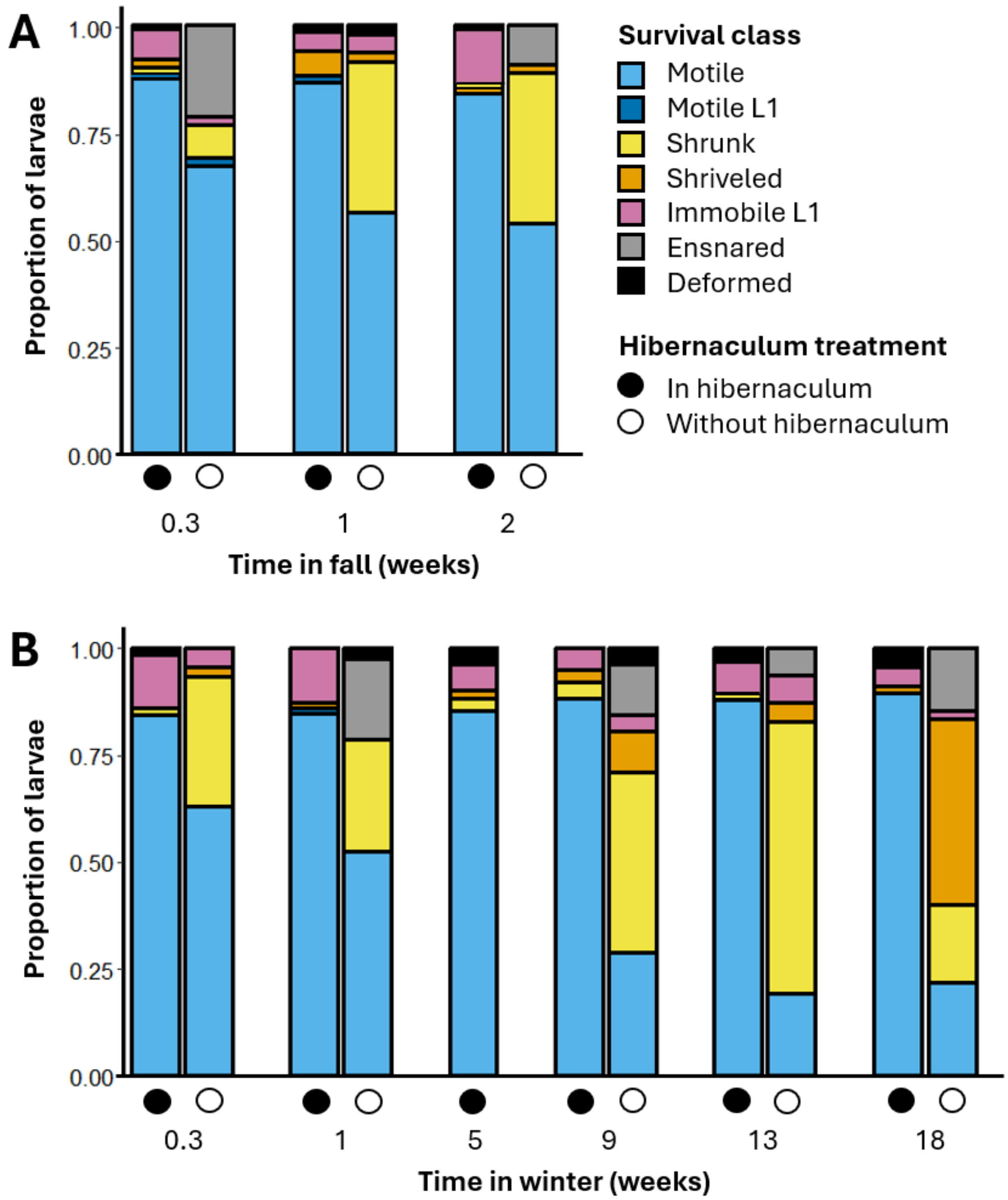

Figure 3.8. Proportion of larvae categorized as one of seven survival classes that were either removed from hibernaculum (○) at day 0 or remained in hibernaculum (●) until classification. **A)** Larvae in fall conditions (20 °C and 16:8 h Light:Dark). **B)** Larvae in winter conditions (2 °C and total darkness) following 17 days of fall conditions. Survival classes consisted of second-instar larvae (Fig. 2.4), unless specified as first-instar (L1). All assessments were conducted at room temperature (ca. 22 °C). Each replicate for budworm without hibernacula contained 50 larvae while each replicate for budworm in hibernacula contained ≥ 50 larvae.

Larval Dispersal Following an IPQL-like Fall & Winter Simulation

Budworm that remained in hibernacula throughout the simulated fall and overwintering conditions showed a higher incidence of dispersal post-winter than budworm that were removed from hibernacula before or during the simulated conditions (Fig. 3.9). The proportion of dispersed larvae remained relatively consistent within a single hibernaculum treatment (early removal, time-specific removal, or no removal; Fig. 3.9). 40% of larvae with no hibernaculum-removal dispersed, while the proportion of dispersed larvae with early or time-specific hibernaculum removal was less than 20% (Fig. 3.9).

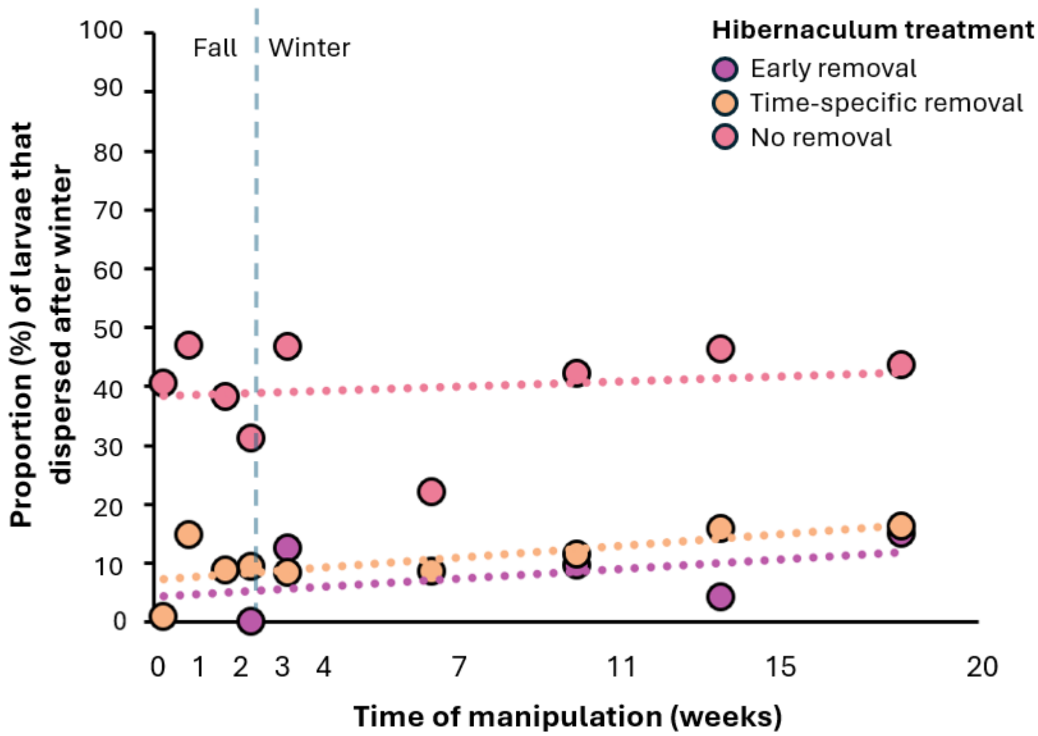

Figure 3.9. Proportion of larvae from one tube that dispersed during a 5-week window following a fall and overwintering simulation. Fall conditions (20 °C and 16:8 h Light:Dark; left of vertical dashed line) lasted 17 days, followed by 126 days of winter conditions (2 °C and total darkness; right of vertical dashed line), and dispersed under the same temperature and photoperiod as fall conditions. Time of manipulation reflects the week at which one group of larvae were transferred from fall or winter conditions to room temperature (ca. 22 °C) for 24 h and then returned to the simulation. For the time-specific removal group (orange), this manipulation involved removal from hibernaculum at the time indicated. For larvae that had hibernacula removed prior to fall conditions (represented in purple) or larvae that remained in hibernacula (pink) for the full simulation, the larvae were simply moved to room temperature for the same duration as the time-specific removal. Each tube from the early removal group contained 50 larvae. Each tube from the time-specific or no removal groups contained ≥ 50 larvae.

Chapter 4: Discussion

To examine an early-diapause temperature-sensitive process, I characterized changes in gene expression and survival associated with cool and warm fall temperature exposures. In addition, because all budworm had their hibernacula removed for these experiments, I tested the effect of this manipulation. According to my initial hypothesis, an unknown temperature-sensitive process occurs during the beginning of budworm diapause, which I predicted would complete later in cool fall conditions and earlier in warm fall conditions. A principal component analysis (PCA) supported my hypothesis, where gene expression of larvae in the early warm fall overlapped with larvae in the late cool fall. Of eight gene profile clusters, some followed a temperature-dependent expression pattern as I originally predicted, while others were temperature-independent or appeared to primarily respond to warm fall conditions. The low warm fall survival, as indicated by the proportion of motile larvae, and removal of hibernacula may also have influenced the PCA and gene clusters. I will describe these patterns in more detail in the following section.

Broad Patterns in Gene Expression & Survival

In a PCA, gene expression of larvae in the early warm fall overlapped with larvae in the late cool fall, indicating similarities in biological processes between these groups. Specifically, gene expression after 2 weeks in the warm fall was equivalent to gene expression across 10 weeks of cool fall conditions, demonstrating possible temperature-dependent diapause development along principal component 2 (PC2). Past research shows that spruce budworm have higher overwintering survival when larvae spend 7-10 weeks in cool fall conditions compared to shorter exposures (Roe et al., 2024). Overall, this suggests that transcriptomic processes that occur late in the cool fall occur at a faster rate in the warm fall, which may drive their temperature-dependent diapause development, as I initially hypothesized. The late warm fall groups that separated along principal component 1 (PC1) likely differed because of prolonged (> 2 weeks) warm fall temperatures, perhaps causing stress and higher mortality. These findings line up with past research, where *C. fumiferana* larvae in warm fall temperatures deplete energy reserves in the form of glycogen over time, lowering their overwintering survival (Roe et al., 2024).

The initiation, maintenance, and termination of spruce budworm diapause have yet to be defined as distinct phases, as exemplified by *C. costata* (Koštál et al., 2017), but this thesis may offer some insights into its timing. Based on gene expression trajectories, it appears that budworm need two weeks in a warm fall to upregulate certain circadian rhythm genes, hormones, *Cf*AFPs, *Cf*HSPs, and antioxidants. Conversely, budworm needed 7-10 weeks to show similar expression patterns in the cool fall. While this points to temperature as a predictor of diapause timing, diapause preparations and initiation were likely already ongoing at the beginning of these fall simulations or had happened beforehand. Emerging research shows that differential gene expression between diapausing and non-diapausing budworm already occurs during the first instar (van der Burg et al., 2024). If so, the second-instar larvae of my experiments may have progressed to a state of diapause maintenance, perhaps when changes in gene expression occur after 2 weeks in the warm fall or 7-10 weeks in the cool fall.

Differentially expressed genes formed eight distinct gene profile clusters (A-H), which demonstrated different types of responses to fall temperatures, including temperature-dependent progression. While clusters A and B both increased gene expression over time, cluster A genes only increased in response to the warm fall temperature. Cluster A's synergy with PC1 further supports that these genes were associated with prolonged heat exposure (> 2 weeks at 20 °C) rather than diapause processes. Cluster B genes showed a less pronounced increase in the late cool fall relative to the warm fall. Clusters C and D showed gene expression peaking after 2 weeks of warm fall or 7-10 weeks of cool fall conditions, supporting the hypothesis that budworm diapause development is temperature-dependent. Of all clusters, cluster C overlapped the most with PC2, strengthening the possibility that these genes drive diapause processes. In clusters E and F, gene expression remained level at first before dropping, where the drop happened after 2 weeks in the warm fall or 7 weeks in the cool fall. This drop could represent a temperature-dependent decrease. However, the decline of the fall cool fall for both clusters is subtle compared to the warm fall. While E and F may fit my initial prediction, cluster G contradicted it, demonstrating temperature-independent gene expression over time in both fall simulations. Cluster H followed a similar downward trajectory, although expression levels declined more in the warm relative to the cool fall. In following chapter sections, I will elaborate on temperature-dependent gene expression in arrested development, metabolic restructuring, and stress tolerance.

Moreover, GO enrichment of several biological processes points to active changes in gene expression during early spruce budworm diapause. Clusters B, C, E, G, and H had 2-4 significant GO terms, while clusters A, D, and F included 6-11 significant terms. Similar to first- and second-instar larvae during the first five days of their respective life stages (van der Burg et al., 2024), terms related to RNA transcription were also enriched in the experiments of this thesis. Gene activity related to these terms increased at the beginning of fall followed by a temperature-delayed decrease (clusters C, D, and F), which supports the idea that many changes may take place during early diapause.

Across the fall simulations, the proportion of motile larvae decreased mainly in response to warm temperatures, suggesting higher lethality in prolonged warm fall exposures. However, mRNA abundance still increased after 10 weeks of warm fall, indicating that genes could still be expressed in at least some individuals. Considering that our Animal Care facility had lower relative humidity (20–50%) during fall simulations than typical IPQL rearing conditions (55±10%; GLFC, 2015), this likely played into low survival during the warm fall. Compared to pre-winter first-instar and post-winter second-instar larvae at 18 °C, budworm in winter conditions (2 °C) retain more water content when exposed to desiccation-drying treatments (Bauce & Han, 2001). Additionally, budworm dried at 2 °C are more desiccation resistant than those dried at 18 °C, after single or multiple one- or two-week treatments (Bauce & Han, 2001). If desiccation resistance is higher in budworm during winter conditions, perhaps larvae in fall conditions are more susceptible to dry out, especially at 18-20 °C.

As all budworm in the fall transcriptome time series experienced hibernaculum-removal during experimental set-up, the question of the hibernaculum's possible effect on motility and gene expression led to a separate fall and overwintering simulation. In this simulation, larvae with intact hibernaculum consistently had a higher proportion of motility and dispersal than larvae removed from their hibernacula, regardless of time of removal. These findings suggest that the hibernaculum plays a role in budworm overwintering survival, at least during early diapause, as larvae that have their hibernacula removed a month into winter conditions have high post-winter survival (Marshall & Sinclair, 2015).

As transcriptomic signals of silk-spinning contributed to PC2 and cluster C, I will elaborate on the possible implications of the hibernaculum later in this chapter. Taking this into consideration, the removal of the hibernaculum presents a limitation of the transcriptomic findings, as the experimental larvae of the transcriptomic time series experienced additional stress from handling (Marshall & Roe, 2021). That being said, spruce budworm in two weeks of warm (20 °C) fall conditions followed by 18 weeks of winter (2 °C) conditions had about 40% overwintering survival (Roe et al., 2024), similar to the proportion of dispersed larvae in the hibernaculum experiment of this thesis. Then, as budworm in the hibernaculum experiment had high motility and similar dispersal, motility is likely a good indicator of overwintering survival.

Another limitation of this thesis lies in the transcriptomic data itself, as gene expression does not accurately reflect an organism's current physiology. While gene expression changes over the course of a time series experiment, translation from RNA to protein is not instantaneous, and mRNA abundance does not mirror protein abundance (Evans, 2015). Furthermore, feedback between transcription and mRNA decay factors dictates the stability of mRNA, and may influence changes in mRNA abundance (Haimovich et al., 2013). Although the RNA libraries of budworm from the fall simulations passed quality control and mapped well to the reference genome, the findings of this thesis remain exploratory in nature. In my analysis, I used patterns in mRNA abundance to identify potential genes that may be relevant for temperature-dependent diapause expression, which future studies can further evaluate in metabolomic, proteomic, or other physiological experiments.

Temperature-Dependent Gene Expression Associated with Fall Diapause Development of the Spruce Budworm

Processes that May Arrest Development in Spruce Budworm Diapause

Expression of photoreceptive genes during early diapause may aid larvae in perceiving environmental cues that lead to developmental arrest. Previous research shows that photoreceptive genes are upregulated in early spruce budworm diapause when compared to a non-diapausing strain (van der Burg et al., 2024). However, I only detected one differentially expressed photoreceptive gene coding for a retinin-like protein that was highly expressed in early fall and downregulated over time at both warm and cool temperatures (cluster G). In *Drosophila melanogaster*, the retinin-like protein serves as a building block for the fruit fly eye's cornea (Kim et al., 2008).

The *timeless* and *daywake* circadian rhythm genes, which could be linked to hormonal control in the developmental arrest of diapause (Ahmadi et al., 2021; Liao et al., 2024), peaked in mRNA abundance early in the warm fall and later in the cool fall (cluster D). While circadian clock genes are typically thought to regulate day-night cycles, they also serve a role in seasonal physiology by responding to photoperiodic cues (Hidalgo & Chiu, 2023). In lepidopterans, this is exemplified by the upregulation of *timeless* in *S. ocellatella* and downregulation of *daywake* in the cabbage butterfly *P. rapae* during diapause initiation (Ahmadi et al., 2021; Liao et al., 2024). Notably, the daywake protein has an "anti-siesta" function that prevents midday sleep in *D. melanogaster* (Yang & Edery, 2019). Perhaps a future experiment could examine whether *daywake* expression is related to decreased motility, or increased "siesta" behaviour, during budworm diapause.

In other lepidopterans, circadian rhythm genes interact with PTTH to release ecdysteroids during diapause initiation, while ecdysteroids can be suppressed by juvenile hormones (JH) to mediate developmental arrest (Ahmadi et al., 2021; Liao et al., 2022; Li et al., 2018). In *C. fumiferana*, increases of JH activate the JH esterase gene, an enzyme that metabolizes JHs to reduce their concentration (Kethidi et al., 2004; Kamita & Hammock, 2010). In fall conditions, JH enzymes and related proteins were differentially regulated in several ways (clusters A, C, D, F, and G). One ecdysone-related gene was highly expressed at the start of fall, which was downregulated more rapidly in the warm than cool fall (cluster H). Considering that many JH-related genes were expressed in several conflicting clusters, perhaps these hormones were tissue-specific, expressed differently prior to the start of the fall simulations, or not relevant to diapause development.

As predicted, multiple genes involved in cell cycle regulation that may contribute to developmental arrest during budworm diapause were differentially regulated in a temperature-dependent manner, including *PCNA* and the cell signalling pathways Wnt and Notch. In *A. glabripennis*, larvae repress genes involved with Wnt signalling during diapause in the Malpighian tubules and midgut while promoting some signalling in the fat body and brain (Torson et al., 2023). As my RNA extractions required a pool of second-instar larvae, it was not possible to distinguish between gene expression in different body parts. But, overall, two Wnt-related genes—encoding for protein Wnt-1 and the homologous transmembrane protein 181—ultimately decreased in response to warm fall conditions (clusters D and F). While gene expression appeared to drop in these clusters at the end of the cool fall, Wnt signalling was seemingly repressed more effectively in the warm fall, which could lead to slower growth and cell proliferation. Notch signalling suppresses cell proliferation during the dormancy of nematodes and killifish but this pathway is not commonly reported in studies on insect diapause, to my knowledge (Karp, 2021). However, the onion fly (*Delia antiqua*) upregulates genes involved in Notch signalling during its pupal summer diapause relative to non-diapausing pupae (Hao et al., 2016). As the GO term for Notch signalling was enriched in cluster D, this pathway could help regulate temperature-dependent diapause development in the spruce budworm alongside Wnt signalling. Lastly, *C. costata* downregulate *PCNA* during cell cycle arrest (Košťál, 2009), which also decreased in *C. fumiferana* after a short warm period or a longer cool period, as in cluster D. Ultimately, cell proliferation may have decreased while cell cycle arrest may have increased at a faster rate in the warm fall through mechanisms of *PCNA* or Wnt and Notch signalling, suggesting developmental arrest occurs faster at warm temperatures than cool temperatures.

Metabolic Restructuring in Spruce Budworm Diapause

In insects, the insulin signalling pathway is involved in both growth and metabolism, and is suggested to aid the accumulation of lipid reserves during diapause (Hahn & Denlinger, 2011; Sim & Denlinger, 2008). There were two changes in gene expression that suggested decreased insulin signalling: an insulin-like peptide decreased in expression during a 10-week fall regardless of temperature (cluster G), possibly reducing the presence of insulin-like peptides and consequent insulin signalling activity (Hahn & Denlinger, 2011). Secondly, the expression of an insulin-degrading enzyme increased in the warm fall (cluster A), possibly reducing insulin signalling. Meanwhile, insulin-like growth factor binding proteins (IGFBPs) were expressed in multiple, perhaps conflicting, clusters (A, F, and H). Since IGFBPs bind to insulin-like peptides, their expression could affect the availability of such peptides (Nässel & Broeck, 2016). Perhaps different IGFBPs serve different functions in different tissues of *C. fumiferana*, which were not captured by the whole-body RNA extractions of this experiment.

Some diapausing insects sequester lipid reserves in preparation for winter diapause (Hahn & Denlinger, 2011), and genes encoding for lipid and fatty acid metabolism were present in PC2 (early diapause-associated) and three gene clusters of my analysis. I originally predicted that *C. fumiferana* larvae would preserve fatty acids and reduce lipid catabolism to conserve limited fat reserves while in a non-feeding phase of their life cycle. For example, diapausing *A. albopictus* larvae have ca. 30% more lipid reserves than non-diapausing larvae (Reynolds et al., 2012). In spruce budworm, lipids in the form of triglyceride drops between fall (18 °C) and winter (2 °C) conditions, but remain at consistent levels during overwintering (Han & Bauce, 1993). During low winter temperatures, the spruce budworm may not be able metabolize lipids, as freezing temperatures rigidify fats and make them energetically inaccessible (Marshall & Roe, 2021; Enriquez & Teets, 2025). However, the maintenance of such reserves could still be useful during fall diapause entry or spring emergence, and may explain why these genes contribute to PC2 in fall (Marshall & Sinclair, 2018). Furthermore, apolipophorins, which mobilize lipids, and lipase 1, which breaks down lipids, both contributed to PC2 (Van der Horst & Ryan, 2012). Meanwhile, Acyl-CoA Delta-9 and -11 desaturases varied in a temperature-dependent manner during diapause. In *A. albopictus*, diapausing larvae downregulated one desaturase gene (Reynolds et al., 2012). In this thesis, delta-11 desaturases were downregulated in the warm fall (cluster F), perhaps serving a different role during early diapause.

Typically, budworm convert glycogen to glycerol for cryoprotection during overwintering (Han & Bauce, 1993; Marshall & Sinclair, 2015), but glycogen can also be tapped into as a carbohydrate storage used for energy (Kihara et al., 2009; Roe et al., 2024). In this thesis, expression of the gene *glycogenin-1* was highest at the beginning of the warm fall simulation, and followed the same downward trajectory for budworm in both warm and cool falls (cluster G). Glycogenin is an enzyme that stimulates glycogen synthesis (Tolmasky et al., 2001), so its downregulation suggests that glycogen synthesis is inhibited in early diapause. This aligns with previous findings showing that budworm have the highest glycogen content after hatching, which decreases rapidly during one week of rearing conditions (23 °C) and two weeks of fall conditions (18 °C) (Han & Bauce, 1993).

Lastly, diapause-associated protein 1 (*Cf*DAP1) was prevalent throughout fall in spruce budworm larvae, congruent with previous studies (Palli et al., 1998; Han et al., 2003). In the results of this thesis, the gene encoding *Cf*DAP1 was highly expressed by budworm on day 0, and decreased over time but mRNA remained abundant (> 200,000 read counts). *Cf*DAPs have a structural similarity to storage proteins called hexamerins, and are highly expressed in two non-feeding stages: diapausing second-instar larvae and pupae (Palli et al., 1998). When deprived of food for one week, homologous proteins to *Cf*DAP are also accumulated by *Choristoneura occidentalis* second-instar larvae of the same genus, suggesting DAP's importance in non-feeding states (Han et al., 2003).

Stress Tolerance Mechanisms Increase in Spruce Budworm Diapause

Of the 16 previously identified *Cf*AFPs (Béliveau et al., 2022), two were expressed in a temperature-dependent manner during spruce budworm early diapause, which may support cold tolerance during later winter conditions. Both *Cf*AFP-15 and -16 were present in cluster C (higher in cool fall conditions) and contributed to PC2 (early diapause-associated). In past studies, first- and second-instar larvae expressed higher levels of *Cf*AFPs during fall (23 °C) or winter (2-4 °C) conditions, followed by a decline when returned to 23 °C post-winter (Qin et al., 2007). Thus, fall gene expression of *Cf*AFPs in my simulations may indicate that budworm begin the process of accumulating these proteins in anticipation of low winter temperatures. Other larvae that diapause, such as *T. granarium*, also express higher levels of AFP gene expression during a 1-week pre-diapause period, demonstrating possible accumulation of AFPs prior to the following 9-week of diapause (Dageri et al., 2023). Furthermore, high expression of *Cf*AFPs during the beginning of the budworm's second instar is congruent with past research, where *Cf*AFP-11 and -13 were highly expressed by first- and second-instar budworm (Béliveau et al., 2022).

Genes related to the metabolism of glycerol, a prominent cryoprotectant in *C. fumiferana* (Han & Bauce, 1995; Marshall & Roe, 2021), were expressed during the fall simulations but not in a temperature-dependent progression. In previous research, larvae exposed to cool (10 °C) temperatures had higher glycerol content than larvae exposed to warm (20 °C) temperatures across fall simulations varying from 0 to 10 weeks (Roe et al., 2024). Furthermore, diapause-destined first- and second-instar budworm demonstrate a continuous upregulation of glycerol synthesis genes compared to their non-diapausing counterparts (van der Burg et al., 2024). In the experiment of this thesis, glycerol kinases increased gene expression in the warm fall (cluster A) and glycerol-3-phosphate (G3P) dehydrogenase decreased expression in the warm fall (cluster E). Glycerol kinase catalyzes the conversion of glycerol to G3P, while G3P dehydrogenase interconverts G3P and a glycolytic intermediate (DHAP) (Blanco & Blanco, 2017; Marshall & Roe, 2021). The changes in expression of these two enzymes suggests that larvae in warm fall conditions are less likely to accumulate glycerol from carbohydrate sources (e.g., glucose undergoing glycolysis) than larvae exposed to cool fall conditions, aligning with glycerol measurements in Roe et al. (2024).

Of the 14 previously identified small *Cf*HSPs (Quan et al., 2018a), five had relatively high expression in early diapause, of which two displayed higher expression late in the cool fall and may support overwintering stress tolerance. Although genes encoding for HSPs were not present in the PCA or gene clusters, *Cf*HSP19.2, 19.6, and 19.7 all increased expression levels in the warm fall and remained stable in the cool fall, indicating that these proteins may primarily respond to prolonged heat (20 °C) exposure. In contrast, *Cf*HSP21.3 and *Cf*HSP24.3 increased gene expression in the cool fall and are consequently associated with the best overwintering survival (Roe et al., 2024). Both proteins may be good targets for investigating the role of small HSPs in cold tolerance. *Cf*HSP24.3 could be of particular interest as it is most highly expressed at the larval stage, while most *Cf*HSPs have higher expression values in the adult stage (Quan et al., 2018a). Additionally, *Cf*HSP24.3 was high in larvae that underwent a 3-week fall (23 °C) and 25-week winter (4 °C) relative to other *Cf*HSPs, but not post-winter, further underlining a possible function during diapause (Quan et al., 2018b).

Gene expression of antioxidants demonstrated possible temperature-dependent progression (clusters D, E, and F), which may help protect against oxidative stress during winter. Insects may employ antioxidants that react with reactive oxygen species to prevent cellular damage (Felton & Summers, 1995). Such is the case for the goldenrod gall moth, *Epiblema scudderiana*, a freeze-avoidant totricid like *C. fumiferana*, which increases antioxidant activity during its larval overwintering stage (Joanisse & Storey, 1996). Antioxidants differentially expressed in spruce budworm included peroxiredoxin-6, catalase, glutathione S-transferase (GST), and superoxide dismutase, of which the latter two were encoded for by multiple genes. As mRNA abundance for most of these antioxidant genes decreased after two weeks in a warm fall and seven weeks in a cool fall, antioxidant synthesis in early diapause may have occurred in preparation for harsh seasonal conditions. In *O. nubilalis*, catalase and glutathione S-transferase had higher enzyme activity in non-diapausing compared to diapausing larvae (Jovanović-Galović et al., 2004). Conversely, both catalase and superoxide dismutase had higher mRNA abundance in adult diapausing *C. pipiens* (Sim & Denlinger, 2011). Glutathione S-transferase and catalase have also been identified in diapausing lepidopteran pupae, namely the silkworm, *Antheraea mylitta,* and the cotton bollworm, *Helicoverpa armigera* (Sahoo et al., 2018; Zhang et al., 2013). All taken into consideration, it is possible that antioxidants contribute to the spruce budworm's stress tolerance during diapause.

Spruce budworm larvae differentially expressed three genes with antimicrobial properties during the fall simulations, pointing to a potentially strengthened immune system in diapause. The three genes—encoding for Attacin-A, Hyphancin-3E, and Diapausin—influenced PC2 (early diapause-associated) and appeared in two clusters. Both attacins and hyphancins have immune system functions in another lepidopteran, the fall webworm, *Hyphantria cunea* (Park et al., 1998; Kwon et al., 2008). The contribution of Hyphancin-3E gene expression in PC2 indicates a possible significance in diapause, although it was not associated with a particular cluster of differential gene expression. In *H. cunea*, Attacin-A is primarily expressed by pupae, which coincidentally is also its diapausing stage (Kwon et al., 2008; Chen et al., 2014). Spruce budworm primarily increased Attacin-A expression in the warm fall (cluster B). Diapausin followed the opposite trend, as in cluster F, where expression in the warm fall decreased. The leaf beetle *Gastrophysa atrocyanea* deploys Diapausin peptides to counter fungal infections (Tanaka et al., 2003). While linked to this beetle's adult diapausing stage, other species—like *M. sexta*, which does not diapause until its pupal stage—employ Diapausin peptides as larvae (Al Souhail et al., 2016). Then, perhaps the link between diapause development and Diapausin peptides is coincidental, although Diapausin still appeared to be influenced by temperature during fall simulations. Overall, the three immune system genes appear relevant for budworm diapause.

The Role of the Hibernaculum in Budworm Fall & Winter Diapause

While integral to the spruce budworm's overwintering, the exact function of the hibernaculum remains unclear (Harvey, 1957). As the hibernaculum provides a physical barrier around the larva, it likely prevents direct contact with ice and consequent ice formation within the insect (Danks, 2004; Marshall & Roe, 2021). Furthermore, the hibernaculum secures the larva to its host tree, so that it remains near its food source upon spring emergence. In my research, I found that hibernaculum presence increased overwintering survival, where I inferred survival from the proportion of motile and dispersed larvae. Since the larvae in this experiment were not exposed to ice or freezing temperatures, there may be another, perhaps unknown, function of the hibernaculum that increases the spruce budworm's overwintering survival.

Based on observations in this study, one can speculate if the hibernaculum's absence causes physiological changes associated with desiccation resistance or cold hardening, as in other overwintering insects that do not form a hibernaculum. For example, the Arctic springtail (*Megaphorura arctica*) employs cryoprotective dehydration to survive cold temperatures, where water loss reduces the possibility of internal freezing (Clark et al., 2009). Hibernaculum-free budworm in this thesis experienced an arguably similar change in physical appearance to dehydrated *M. arctica* (see Clarke et al., 2009), as the incidence of "shrunken"-looking larvae increased throughout fall and winter. However, previous research indicates that the hibernaculum does not prevent water loss in *C. fumiferana* (Bauce & Han, 2001). In the former study, second-instar larvae lost about 40% of water content when desiccant-dried for two weeks at 18 °C, regardless of the presence or absence of hibernacula (Bauce & Han, 2001).

Several potentially hibernaculum-associated genes were differentially expressed in this study, including those involved in silk-spinning and cuticle composition. The silk of *B. mori* is composed of fibroin proteins glued together by sericin proteins (Mondal et al., 2007). Additional silk proteins called seroins also have antimicrobial properties, able to counter viral and bacterial infections in *B. mori* (Singh et al., 2014; Dong et al., 2023). In spruce budworm larvae, an uncharacterized seroin-like gene had the highest contribution to PC2 overall. The gene expression of three other seroin and fibroin proteins were detected in PC2 and cluster C. Considering that the larvae in question were removed from their hibernacula at the beginning of the experiment, it is possible that they attempted to re-spin hibernacula, hence the activity of these genes. In my personal observations during the experiment, I saw that a few budworm removed from their hibernacula attempted to spin a new one within the tube, which at times resulted in entanglements of larvae. That being said, the temperature-dependent progression of these genes points to the possibility that silk-spinning is part of the spruce budworm's diapause response.

The high contribution of cuticular proteins to PC2 could also be interlinked with hibernaculum spinning (Qi & Liu, 2025). Cuticular proteins tend to have life stage- and tissue-specific gene expression and provide support for different insect structures, including silk glands (Qi & Liu, 2025). In *B. mori*, a majority of genes encoding for cuticular synthesis were upregulated in the anterior part of its glands, which is the part of the gland structure where silk proteins are solidified (Chang et al., 2015). Cuticular proteins in spruce budworm could perform similar functions. However, other cuticle proteins—such as the tweedle family—have been implicated in the cold and hypoxia tolerance of *Drosophila suzukii* fly larvae (Wang et al., 2023). One such gene, tweedleT, was the third most influentially expressed gene in PC2. Then, considering the multitude of cuticular genes in PC2 and the physical changes across the fall simulations, it is possible that these proteins had several different functions and responded to tissue-specific restructuring that was not captured by the whole-body RNA extractions. For example, expression of genes like tweedleT may result from temperature stress, while others may have a specific role in silk glands.

Conclusions & Future Directions

Originally, I had hypothesized that an unknown temperature-sensitive process occurs during the beginning of budworm diapause, and that this process would complete later in cool fall conditions and earlier in warm fall conditions. In this thesis, I showed that budworm expressed genes related to several diapause-related processes in a temperature-dependent manner. Overall, temperature-dependent patterns were more prominent in features of arrested development and stress tolerance rather than metabolic restructuring. Changes in metabolism—such as insulin signalling or the breakdown of lipids and glycerol—were more so influenced by warm falls.

As demonstrated in this thesis, the relationship between the hibernaculum and overwintering survival is complex, where motility appeared mediated by the warm fall while silk-spinning genes were expressed in a temperature-dependent manner. Altogether, it seems that hibernaculum formation and diapause response could be intertwined in some way that is yet to be fully understood. A future study may build on these findings to re-evaluate the role of dehydration in warm falls, the contribution of cuticular proteins to spruce budworm silk glands, and the question of the hibernaculum's antimicrobial properties.

The timing of developmental events during budworm diapause and genes associated with diapause phases and transitions have yet to be documented. To better understand the timing of changes in diapause development, a time series which incorporates first-instar larvae will be necessary. Some possible candidates for further study are Notch signalling genes, the circadian rhythm gene *daywake*, *Cf*AFPs, *Cf*HSP24.3, and seroin- and fibroin-related genes, all of which appeared relevant to spruce budworm diapause in this thesis. Additional gene expression, survival, or other physiological data from overwintering budworm may also help our understanding of their diapause maintenance, termination, and possibly post-diapause quiescence.

References

Ahmadi, F., Mikani, A., & Moharramipour, S. (2021). Induction of diapause by clock proteins period and timeless via changes in PTTH and ecdysteroid titer in the sugar beet moth, *Scrobipalpa ocellatella* (Lepidoptera: Gelechiidae). *Insect Biochemistry & Physiology*, *107*(2). https://doi.org/10.1002/arch.21790

Alexa, A., & Rahnenfuhrer, J. (2022). topGO: Enrichment analysis for Gene Ontology. R package version 2.50.0. https://doi.org/10.18129/B9.bioc.topGO

Al Souhail, Q., Hiromasa, Y., Rahnamaeian, M., Giraldo, M. C., Takahashi, D., Valent, B., Vilcinskas, A., & Kanost, M. R. (2016). Characterization and regulation of expression of an antifungal peptide from hemolymph of an insect, *Manduca sexta*. *Developmental and Comparative Immunology, 61*, 258-268. https://doi.org/10.1016/j.dci.2016.03.006

Anders, S. Pyl, P. T., & Huber, W. (2015). HTSeq—a Python framework to work with high-throughput sequencing data. *Bioinformatics*, *15;31*(2), 166-9. https://doi.org/10.1093/bioinformatics/btu638

Andrews, S. (2010). FastQC: A quality control tool for high throughput sequence data. https://www.bioinformatics.babraham.ac.uk/projects/fastqc/

Bauce, É., & Han, E.-N. (2001). Desiccation resistance in pre-diapause, diapause and post-diapause larvae of *Choristoneura fumiferana* (Lepidoptera: Tortricidae). *Bulletin of Entomological Research, 91*(5), 321-326. https://doi.org/10.1079/BER2001119

Béliveau, C., Gagné, P., Picq, S., Vernygora, O., Keeling, C. I., Pinkney, K., Doucet, D., Wen, F., Johnston, J. S., Maaroufi, H., Boyle, B., Laroche, J., Dewar, K., Juretic, N., Blackburn, G., Nisole, A., Brunet, B., Brandão, M., Lumley, L., Duan, J., Quan, G., Lucarotti, C. J., Roe, A. D., Sperling, F. A. H., Levesque, R. C., & Cusson, M. (2022). The spruce budworm genome: Reconstructing the evolutionary history of antifreeze proteins. *Genome Biology and Evolution, 14*(6), https://doi.org/10.1093/gbe/evac087

Bellemin-Noël, B., Bourassa, S., Despland, E., De Grandpré, L., & Pureswaran, D. S. (2021). Improved performance of the eastern spruce budworm on black spruce as warming temperatures disrupt phenological defences. *Global Change Biology, 27*(14), 3358-3366. https://doi.org/10.1111/gcb.15643

Blanco, A., & Blanco, G. (2017). *Medical Biochemistry*. Academic Press.

Butterson, S., Roe, A. D., & Marshall, K. E. (2021). Plasticity of cold hardiness in the eastern spruce budworm, *Choristoneura fumiferana*. *Comparative Biochemistry and Physiology, 259*, 110998-110998. https://doi.org/10.1016/j.cbpa.2021.110998

Bolger, A. M., Lohse, M., & Usadel, B. (2014). Trimmomatic: A flexible trimmer for Illumina sequence data. *Bioinformatics*, *30*(15), 2114-2120. https://doi.org/10.1093/bioinformatics/btu170

Candau, J.-N., & Fleming, R. A. (2008). *Forecasting the response to climate change of the major natural biotic disturbance regime in Ontario's forests: The spruce budworm.* (Climate Change Research Report: CCRR-13). https://www.researchgate.net/publication/280101753_Forecasting_the_response_to_climate_change_of_the_major_biotic_disturbance_regime_in_Ontario's_forests_the_spruce_budworm

Chang, H., Cheng, T., Wu, Y., Hu, W., Long, R., Liu, C., Zhao, P., & Xia, Q. (2015). Transcriptomic analysis of the anterior silk gland in the domestic silkworm (*Bombyx mori*) – Insight into the mechanism of silk formation and spinning. *PLOS ONE*, *10*(9). https://doi.org/10.1371/journal.pone.0139424

Chen, C., Wei, X., Xiao, H., He, H., Xia, Q., & Xue, F. (2014). Diapause induction and termination in *Hyphantria cunea* (Drury) (Lepidoptera: Arctiinae). *PLOS ONE, 9*(5). https://doi.org/10.1371/journal.pone.0098145

Chen, J.-j., Liu, X.-x., Guo, P.-h., Teets, N. M., Zhou, J.-C., Chen, W.-b., Luo, Q.-z., Kanjana, N., Li, Y.-y., & Zhang, L.-s. (2024). Regulation of forkhead box O transcription factor by insulin signaling pathway controls the reproductive diapause of the lady beetle, *Coccinella septempunctata*. *International Journal of Biological Macromolecules, 258*(1), https://doi.org/10.1016/j.ijbiomac.2023.128104

Clark, M. S., Thorne, M. A. S., Purać, J., Burns, G., Hillyard, G., Popović, Ž. D., Grubor-Lajšić, G., & Worland, M. R. (2009). Surviving the cold: Molecular analyses of insect cryoprotective dehydration in the Arctic springtail *Megaphorura arctica* (Tullberg). *BMC Genomics, 10.* https://doi.org/10.1186/1471-2164-10-328

Clarke, A. (1993). Seasonal acclimatization and latitudinal compensation in metabolism: Do they exist? *Functional Ecology, 7*(2), 139-149. https://doi.org/10.2307/2389880

Conesa, A., & Nueda, M. J. (2024). Significant gene expression profile differences in time course gene expression data. R package version 1.76.0.

Dageri, A., Kadir, M. L., Guz, N., Ogreten, A., & Arshad, M. (2023). The involvement of Antifreeze protein maxi-like and Cold-shock domain-containing protein genes in cold-induced larval diapause and cold-shock treatment of khapra beetle. *Journal of Stored Products Research*, *101*. https://doi.org/10.1016/j.jspr.2022.102074

Danks, H. V. (2004). The roles of insect cocoons in cold conditions. *European Journal of Entomology*, *101*. 433-437.

Denlinger, D. L. (2022). *Insect diapause*. Cambridge University Press. https://doi.org/10.1017/9781108609364

Denlinger, D. L. (2023). Insect diapause: From a rich history to an exciting future. *Journal of Experimental Biology*, *226*(4). https://doi.org/10.1242/jeb.245329

Dong, Z., Xia, Q., & Zhao, P. (2023). Antimicrobial components in the cocoon silk of silkworm, *Bombyx mori*. *International Journal of Biological Macromolecules, 224*, 68-78. https://doi.org/10.1016/j.ijbiomac.2022.10.103

Dowle, E. J., Powell, T. H. Q., Doellman, M. M., Meyers, P. J., Calvert, M. B., Walden, K. K. O., Robertson, H. M., Berlocher, S. H., Feder, J. L., Hahn, D. A., & Ragland, G. J. (2020). Genome-wide variation and transcriptional changes in diverse developmental processes underlie the rapid evolution of seasonal adaptation. *PNAS, 117*(38), 23960-23969. https://doi.org/10.1073/pnas.2002357117

Duplouy, A., Minard, G., Lähteenaro, M., Rytteri, S., & Saastamoinen, M. (2018). Silk properties and overwinter survival in gregarious butterfly larvae. *Ecology & Evolution*, *8*(24), 12443-12455. https://doi.org/10.1002/ece3.4595

Enriquez, T., & Teets, N. M. (2024). Lipid properties and metabolism in response to cold. In Rezaei, N., Steinlein, O., Rosenhouse-Dantsker, A., & Gerlai, R. (Eds.), *Advances in Experimental Medicine and Biology*. Springer, Cham. https://doi.org/10.1007/5584_2024_848

Evans, T. G. (2015). Considerations for the use of transcriptomics in identifying the 'genes that matter' for environmental adaptation. *Journal of Experimental Biology*, *218*(12), 1925-1935. https://doi.org/10.1242/jeb.114306

Ewels, P., Magnusson, M., Lundin, S., & Käller, M. (2016). MultiQC: Summarize analysis results for multiple tools and samples in a single report. *Bioinformatics*, *32*(19), 3047-3048. https://doi.org/10.1093/bioinformatics/btw354

Felton, G. W., & Summers, C. B. (1995). Antioxidant systems in insects. *Archives of Insect Biochemistry and Physiology, 29*(2), 187-197. https://doi.org/10.1002/arch.940290208

Great Lakes Forestry Centre (GLFC). (2015). *Rearing diapause* Choristoneura fumiferana *(D*Cf*)* (Standard Operating Procedure: No. IPS/003/003). https://publications.gc.ca/collections/collection_2016/rncan-nrcan/Fo123-4-003-003-2015-eng.pdf

Hahn, D. A., & Denlinger, D. L. (2011). Energetics of insect diapause. Annual Review of Entomology, 56, 103-121. https://doi.org/10.1146/annurev-ento-112408-085436

Haimovich, G., Medina, D. A., Causse, S. Z., Garber, M., Millán-Zambrano, G., Barkai, O., Chávez, S., Pérez-Ortín, J. E., Darzacq, X., & Choder, M. (2013). Gene expression is circular: Factors for mRNA degradation also foster mRNA synthesis. *Cell, 153*(5), 1000–1011. https://doi.org/10.1016/j.cell.2013.05.012

Han, E.-N., & Bauce, E. (1993). Physiological changes and cold hardiness of spruce budworm larvae, *Choristoneura fumiferana* (Clem.), during pre-diapause and diapause development under laboratory conditions. *The Canadian Entomologist, 125*(6), 1043-1053. https://doi.org/10.4039/Ent1251043-6

Han, E.-N., & Bauce, É. (1995). Freeze survival of spruce budworm larvae, *Choristoneura fumiferana*, at subzero temperatures during diapause. *Entomologia Experimentalis et Applicata*, *75*(1), 67-74, https://doi.org/10.1111/j.1570-7458.1995.tb01911.x

Han, E.-N., & Bauce, É. (1998). Timing of diapause initiation, metabolic changes and overwintering survival of the spruce budworm, *Choristoneura fumiferana*. *Ecological Entomology, 23*, 160-167. https://doi.org/10.1046/j.1365-2311.1998.00111.x

Han, E.-N., Béliveau, C., Bauce, É., & Cusson, M. (2003). Effect of starvation on the accumulation of *Cf*DAP and *Cf*DAP-like proteins in post-diapause *Choristoneura fumiferana* and diapause-free *Choristoneura occidentalis*. *Canadian Journal of Zoology, 81*(2), 335-339. https://doi.org/10.1139/z03-012

Hao, Y.-J., Zhang, Y.-J., Si, F.-L., Fu, D.-Y., He, Z.-B., & Chen, B. (2016). Insight into the possible mechanism of the summer diapause of *Delia antiqua* (Diptera: Anthomyiidae) through digital gene expression analysis. *Insect Science, 23*(3), 438-451. https://doi.org/10.1111/1744-7917.12323

Harvey, G. T. (1957). The occurrence and nature of diapause-free development in the spruce budworm, *Choristoneura fumiferana* (Clem.) (Lepidoptera: Tortricidae). *Canadian Journal of Zoology, 35*(4), 549-572. https://doi.org/10.1139/z57-047

Harvey, G. T. (1961). Second diapause in spruce budworm from Eastern Canada. *Canadian Entomologist, 93*(7), 594-602. https://doi.org/10.4039/Ent93594-7

Harvey, G. T. (1967). On coniferophagous species of *Choristoneura* (Lepidoptera: Totricidae) in North America: V. Second diapause as a species character. *The Canadian Entomologist*, *99*(5), 486-503. https://doi.org/10.4039/Ent99486-5

Harvey, G. T. (1983). A geographical cline in egg weights in *Choristoneura fumiferana* (Lepidoptera: Tortricidae) and its significance in population dynamics. *The Canadian Entomologist, 115*, 1103-1108. https://doi.org/10.4039/Ent11 51103-9

Hidalgo, S., & Chiu, J. C. (2023). Integration of photoperiodic and temperature cues by the circadian clock to regulate insect seasonal adaptations. *Journal of Comparative Physiology A*, *210*, 585-599. https://doi.org/10.1007/s00359-023-01667-1

Huey, R. B., & Stevenson, R. D. (1979). Integrating thermal physiology and ecology of ectotherms: A discussion of approaches. *American Zoologist*, *19*(1), 357-366. https://doi.org/10.1093/icb/19.1.357

Joanisse, D. R., & Storey, K. B. (1996). Fatty acid content and enzymes of fatty acid metabolism in overwintering cold-hardy gall insects. *Physiological Zoology*, *69*(5), 1079-1095. http://www.jstor.org/stable/30164247

Jones, P., Binns, D., Chang, H.-Y., Fraser, M., Li, W., McAnulla, C., McWilliam, H., Maslen, J., Mitchell, A., Nuka, G., Pesseat, S., Quinn, A. F., Sangrador-Vegas, A., Scheremetjew, M., Yong, S.-Y., Lopez, R., & Hunter, S. (2014). InterProScan 5: Genome-scale protein function classification. *Bioinformatics, 30*(9), 1236-1240. https://doi.org/10.1093/bioinformatics/btu031

Jovanović-Galović, A., Blagojević, D. P., Grubor-Lajšić, G., Worland, R., & Spasićet M. B. (2004). Role of antioxidant defense during different stages of preadult life cycle in European corn borer (*Ostrinia nubilalis*, Hubn.): Diapause and metamorphosis. *Insect Biochemistry and Physiology*, *55*(2), 79-89. https://doi.org/10.1002/arch.10126

Kamita, S. G., & Hammock, B. D. (2010). Juvenile hormone esterase: biochemistry and structure. *Journal of Pesticide Science, 35*(3), 265-274. https://doi.org/10.1584/jpestics.R10-09

Karp, X. (2021). Hormonal regulation of diapause and development in nematodes, insects, and fishes. *Frontiers in Ecology and Evolution, 9*. https://doi.org/10.3389/fevo.2021.735924

Katsoyannos, P., Kontodima, D. C., & Stathas, G. (2005). Summer diapause and winter quiescence of *Hippodamia* (*Semiadalia*) *undecimnotata* (Coleoptera: Coccinellidae) in central Greece. *European Journal of Entomology, 102*(3), 453-457, https://doi.org/10.14411/eje.2005.065

Kethidi, D. R., Perera, S. C., Zheng, S., Feng, Q.-L., Krell, P., Retnakaran, A., & Palli, S. R. (2004). Identification and characterization of a juvenile hormone esterase gene from the spruce budworm, *Choristoneura fumiferana*. *Journal of Biological Chemistry, 279*(19), 19634-19642. https://doi.org/10.1074/jbc.M412406200

Kihara, F., Itoh, K., Iwasaka, M., Niimi, T., Yamashita, O., & Yaginuma, T. (2009). Glycerol kinase activity and *glycerol kinase-3* gene are up-regulated by acclimation to 5 °C in diapause eggs of the silkworm, *Bombyx mori*. *Insect Biochemistry and Molecular Biology, 39*(11), 763-769. https://doi.org/10.1016/j.ibmb.2009.09.001

Kim, D., Paggi, J. M., Park, C., Bennett, C., & Salzberg, S.L. (2019). Graph-based genome alignment and genotyping with HISAT2 and HISAT-genotype. *Nature Biotechnology*, *37*, 907-915. https://doi.org/10.1038/s41587-019-0201-4

Kim, E., Choi, Y., Lee, S., Seo, Y., Yoon, J., & Baek, K. (2008). Characterization of the *Drosophila melanogaster retinin* gene encoding a cornea-specific protein. *Insect Molecular Biology*, *17*(5), 537-543. https://doi.org/10.1111/j.1365-2583.2008.00822.x

Košťál, V. (2000). Induction and development of winter larval diapause in a drosophilid fly, *Chymomyza costata*. *Journal of Insect Physiology, 46*(4), 417-428. https://doi.org/10.1016/S0022-1910(99)00124-9

Košťál, V. (2006). Eco-physiological phases of insect diapause. Journal of Insect Physiology, 52(1), 113-127. https://doi.org/10.1016/j.jinsphys.2005.09.008

Koštál, V., Šimůnková, P., Kobelková, A., & Shimada, K. (2009). Cell cycle arrest as a hallmark of insect diapause: Changes in gene transcription during diapause induction in the drosophilid fly, *Chymomyza costata*. *Insect Biochemistry and Molecular Biology*, *39*(12), 875-883. https://doi.org/10.1016/j.ibmb.2009.10.004

Košťál, V., Štětina, T., Poupardin, R., Korbelová, J., & Bruce, A. W. (2017). Conceptual framework of the eco-physiological phases of insect diapause development justified by transcriptomic profiling. *PNAS, 114*(32), 8532-8537. https://doi.org/10.1073/pnas.1707281114

Kukal, O. (1995). Winter mortality and the function of larval hibernacula during the 14-year life cycle of an arctic moth, *Gynaephora groenlandica*. *Canadian Journal of Zoology*, *73*(4). 657-662. https://doi.org/10.1139/z95-077

Kwon, Y. M., Kim, H. J., Kim, Y. I., Kang, Y. J., Lee, I. H., Jin, B. R., Han, Y. S., Cheon, H. M., & Ha, N. G. (2008). Comparative analysis of two attacin genes from *Hyphantria cunea*. *Comparative Biochemistry and Physiology Part B: Biochemistry and Molecular Biology, 151*(2), 213-220. https://doi.org/10.1016/j.cbpb.2008.07.002

Lebenzon, J. E., Torson, A. S., & Sinclair, B. J. (2021). Diapause differentially modulates the transcriptomes of fat body and flight muscle in the Colorado potato beetle. *Comparative Biochemistry and Physiology Part D: Genomics and Proteomics, 40*. https://doi.org/10.1016/j.cbd.2021.100906

Lebenzon, J. E., Denezis, P. W., Mohammad, L., Mathers, K. E., Turnbull, K. F., Staples, J. F., & Sinclair, B. J. (2022). Reversible mitophagy drives metabolic suppression in diapausing beetles. *PNAS, 119*(30). https://doi.org/10.1073/pnas.2201089119

Li, K., Jia, Q.-Q., & Li, S. (2018). Juvenile hormone signaling: A mini review. *Insect Science*, *26*(4), 600-606. https://doi.org/10.1111/1744-7917.12614

Liao, J., Cai, D., Geng, S., Lyu, Z., Wu, Y., Guo, J., & Li, H. (2024). Transcriptome-based analysis reveals a crucial role of the 20E/HR3 pathway in the diapause of *Pieris rapae*. *Pesticide Biochemistry & Physiology*, *199*. https://doi.org/10.1016/j.pestbp.2024.105787

Liu, E.Y., Lantz, V.A., MacLean, D.A., & Hennigar, C. (2019). Economics of early intervention to suppress a potential spruce budworm outbreak on crown land in New Brunswick, Canada. Forests, 10(6). https://doi.org/10.3390/f10060481

Love, M. I., Huber, W., & Anders, S. (2014). Moderated estimation of fold change and dispersion for RNA-seq data with DESeq2. *Genome Biology, 15*(550). https://doi.org/10.1186/s13059-014-0550-8

Lumley, L. M., Pouliot, E., Laroche, J., Boyle, B., Brunet, B. M. T., Levesque, R. C., Sperling, F. A. H., & Cusson, M. (2020). Continent-wide population genomic structure and phylogeography of North America's most destructive conifer defoliator, the spruce budworm (*Choristoneura fumiferana*). *Ecology and Evolution, 10*(2), 914-927. https://doi.org/10.1002/ece3.5950

MacLean, D. A. (2019). Protection strategy against spruce budworm. *Forests, 10*(12). https://doi.org/10.3390/f10121137

Marshall, K. E., & Sinclair, B. J. (2015). The relative importance of number, duration and intensity of cold stress events in determining survival and energetics of an overwintering insect. *Functional Ecology, 29*(3), 357-366. https://doi.org/10.1111/1365-2435.12328

Marshall, K. E., Gotthard, K., & Williams, C. M. (2020). Evolutionary impacts of winter climate change on insects. *Current Opinion in Insect Science, 41*, 54-62. https://doi.org/10.1016/j.cois.2020.06.003

Marshall, K. E., & Roe, A. D. (2021). Surviving in a frozen forest: The physiology of eastern spruce budworm overwintering. *Physiology, 36*(3), 174-182. https://doi.org/10.1152/PHYSIOL.00037.2020

Martin, M. (2011). Cutadapt removes adapter sequences from high-throughput sequencing reads. *EMBnet.journal, 17*(1), 10-12. https://doi.org/10.14806/ej.17.1.200

McMorran, A. (1965). A synthetic diet for the spruce budworm, *Choristoneura fumiferana* (Clem.) (Lepidoptera: Tortricidae). *The Canadian Entomologist, 97*(1), 58-62. https://doi.org/10.4039/Ent9758-1

Mondal, M., Trivedy, K., and Nirmal Kumar, S. (2007). The silk proteins, sericin and fibroin silkworm, *Bombyx mori* Linn.,—a review. *Caspian Journal of Environmental Science, 5*(2), 63-76.

Moraiti, C. A., & Papadopoulos, N.T. (2017). Obligate annual and successive facultative diapause establish a bet-hedging strategy of *Rhagoletis cerasi* (Diptera: Tephritidae) in seasonally unpredictable environments. *Physiological Entomology*, *42*(3), 225-231. https://doi.org/10.1111/phen.12206

Nässel, D. R., Broeck, J. V. (2016). Insulin/IGF signaling in *Drosophila* and other insects: Factors that regulate production, release and post-release action of the insulin-like peptides. *Cellular and Molecular Life Sciences, 73*, 271-290. https://doi.org/10.1007/s00018-015-2063-3

Overgaard, J., & MacMillan, H. A. (2017). The integrative physiology of insect chill tolerance. *Annual Review of Physiology, 79*, 187-208. https://doi.org/10.1146/annurev-physiol-022516-034142

Palli, S. R., Ladd, T. R., Ricci, A. R., Primavera, M., Mungrue, I. N., Pang, A. S. D., Retnakaran, A. (1998). Synthesis of the same two proteins prior to larval diapause and pupation in the spruce budworm, *Choristoneura fumiferana*. *Journal of Insect Physiology, 44*(5-6), 509-524. https://doi.org/10.1016/S0022-1910(97)00123-6

Park, H. Y., Park, S. S., Park, D. S., Shin, S. W., & Joo, C. K. (1998). Bacteria-induced antibacterial peptide, Hyphancin from the fall webworm, *Hyphantria cunea*. *Korean Journal of Entomology*, *24*(3), 191-198. https://doi.org/10.5555/19961100249

Poupardin, R., Schöttner, K., Korbelová, J., Provazník, J., Doležel, D., Pavlinic, D., Beneš, V., & Koštál, V. (2015). Early transcriptional events linked to induction of diapause revealed by RNAseq in larvae of drosophilid fly, *Chymomyza costata*. *BMC Genomics*, *16*. https://doi.org/10.1186/s12864-015-1907-4

Qi, H., & Liu, T. (2025). Cuticular proteins: Essential molecular code for insect survival. *Insect Biochemistry and Molecular Biology, 184*. https://doi.org/10.1016/j.ibmb.2025.104402

Qin, W., Doucet, D., Tyshenko, M. G., & Walker, V. K. (2007). Transcription of antifreeze protein genes in *Choristoneura fumiferana*. *Insect Molecular Biology*, *16*(4), 423-434. https://doi.org/10.1111/j.1365-2583.2007.00743.x

Quan, G., Duan, J., Ladd, T., & Krell, P. J. (2018a). Identification and expression analysis of multiple small heat shock protein genes in spruce budworm, *Choristoneura fumiferana* (L.). *Cell Stress & Chaperones, 23*(1), 141-154. https://doi.org/10.1007/s12192-017-0832-7

Quan, G., Duan, J., Fick, W., Kyei-Poky, G., & Candau, J.-N. (2018b). Expression profiles of 14 small heat shock protein (sHSP) transcripts during larval diapause and under thermal stress in the spruce budworm, *Choristoneura fumiferana* (L.). *Cell Stress and Chaperones, 23*(6), 1247-1256. https://doi.org/10.1007/s12192-018-0931-0

Ragland, G. J., Fuller, J., Feder, J. L., & Hahn, D. A. (2009). Biphasic metabolic rate trajectory of pupal diapause termination and post-diapause development in a tephritid fly. *Journal of Insect Physiology*, *55*, 344-350. https://doi.org/10.1016/j.jinsphys.2008.12.013

Ragland, G. J., & Keep, E. (2017). Comparative transcriptomics support evolutionary convergence of diapause responses across Insecta. *Physiological Entomology*, *42*(3), 246-256. https://doi.org/10.1111/phen.12193

R Core Team. (2025). R: A Language and Environment for Statistical Computing. R Foundation for Statistical Computing, Vienna, Austria. https://www.R-project.org

Reynolds, J. A., Poelchau, M. F., Rahman, Z., Armbruster, P. A., & Denlinger, D. L. (2012). Transcript profiling reveals mechanisms for lipid conservation during diapause in the mosquito, *Aedes albopictus*. *Journal of Insect Physiology, 58*(7), 966–973. https://doi.org/10.1016/j.jinsphys.2012.04.013

Roe, A. D., Demidovich, M., & Dedes, J. (2018). Origins and history of laboratory insect stocks in a multispecies insect production facility, with the proposal of standardized nomenclature and designation of formal standard names. *Journal of Insect Science, 18*(3). https://doi.org/10.1093/jisesa/iey037

Roe, A. D., Wardlaw, A. A., Butterson, S., & Marshall, K. E. (2024). Diapause survival requires a temperature-sensitive preparatory period. *Current Research in Insect Science, 5*. https://doi.org/10.1016/j.cris.2024.100073

Sahoo, A., Dutta, A., Dandapat, J., & Samanta, L. (2018). Low H_2O_2 and enhanced oxidative resistance in the diapause-destined pupa of silkworm, *Antheraea mylitta* (Lepidoptera:Saturniidae) suggest their possible involvement in dormancy and lifespan extension. *BMC Zoology, 3*(1). https://doi.org/10.1186/s40850-018-0027-4

Sim, C., & Denlinger, D.L. (2008). Insulin signaling and FOXO regulate the overwintering diapause of the mosquito *Culex pipiens*. *PNAS, 105*(18), 6777-6781, www.pnas.org/cgi/doi/10.1073/pnas.0802067105

Sim, C., & Denlinger, D. L. (2011). Catalase and superoxide dismutase-2 enhance survival and protect ovaries during overwintering diapause in the mosquito *Culex pipiens*. *Journal of Insect Physiology, 57*(5), 628-634. https://doi.org/10.1016/j.jinsphys.2011.01.012

Sinclair, B. J., Williams, C. M., & Terblanche, J. S. (2012). Variation in thermal performance among insect populations. *Physiological and Biochemical Zoology, 85*(6), 594-606. https://doi.org/10.1086/665388

Sinclair, B. J., Ferguson, L. V., Salehipour-Shirazi, G., & MacMillan, H. A. (2013). Cross-tolerance and cross-talk in the cold: Relating low temperatures to desiccation and immune stress in insects. *Integrative and Comparative Biology, 53*(4), 545-556. https://doi.org/10.1093/icb/ict004

Singh, C. P., Vaishna, R. L., Kakkar, A., Arunkumar, K. P., & Nagaraju, J. (2014). Characterization of antiviral and antibacterial activity of *Bombyx mori* seroin proteins. *Cellular Microbiology, 16*, 1354-1365. https://doi.org/10.1111/cmi.12294

Sokolova, I. M. (2013). Energy-limited tolerance to stress as a conceptual framework to integrate the effects of multiple stressors. *Integrative & Comparative Biology*, *53*(4), 597-608. https://doi.org/10.1093/icb/ict028

Sponagle, J. (2022, August 24). Nova Scotia prepares for the next spruce budworm outbreak. *CBC*. https://www.cbc.ca/news/canada/nova-scotia/nova-scotia-prepares-spruce-budworm-outbreak-1.6561089

Stehr, G. (1954). A laboratory method for rearing the spruce budworm, *Choristoneura fumiferana* (Clem.), (Lepidoptera: Tortricidae). *The Canadian Entomologist*, *86*(9), 423-428. https://doi.org/10.4039/Ent86423-9

Steward, R. A., Pruisscher, P., Roberts, K. T., & Wheat, C. W. (2024). Genetic constraints in genes exhibiting splicing plasticity in facultative diapause. *Heredity, 132*, 142-155. https://doi.org/10.1038/s41437-024-00669-2

Suang, S., Manaboon, M., Singtripop, T., Hiruma, K., Kaneko, Y., Tiansawat, P., Neumann, P., & Chantawannakul, P. (2017). Larval diapause termination in the bamboo borer, *Omphisa fuscidentalis*. *PLOS ONE*, *12*(4). https://doi.org/10.1371/journal.pone.0174919

Süess, P., Dircksen, H., Roberts, K. T., Gotthard, K., Nässel, D. R., Wheat, C. W., Carlsson, M. A., & Lehmann, P. (2022). Time- and temperature-dependent dynamics of prothoracicotropic hormone and ecdysone sensitivity co-regulate pupal diapause in the green-veined white butterfly *Pieris napi*. *Insect Biochemistry & Molecular Biology*, *149*. https://doi.org/10.1016/j.ibmb.2022.103833

Tanaka, H., Sato, K., Saito, Y., Yamashita, T., Agoh, M., Okunishi, J., Tachikawa, E., & Suzuki, K. (2003). Insect diapause-specific peptide from the leaf beetle has consensus with a putative iridovirus peptide. *Peptides, 24*(9), 1327-1333. https://doi.org/10.1016/j.peptides.2003.07.021

Tolmasky, D.S., Rabossi, A., Quesada-Allué, L.A. (2001). Synthesis and mobilization of glycogen during metamorphosis of the medfly *Ceratitis capitata*. *Archives of Biochemistry and Biophysics, 392*(1), 38-47. https://doi.org/10.1006/abbi.2001.2394

Torson, A. S., Bowman, S., Doucet, D., Roe, A. D., & Sinclair, B. J. (2023). Molecular signatures of diapause in the Asian longhorned beetle: Gene expression. *Current Research in Insect Science, 3*. https://doi.org/10.1016/j.cris.2023.100054

Toxopeus, J., Gadey, L., Andaloori, L., Sanaei, M., & Ragland, G. J. (2021). Costs of averting or prematurely terminating diapause associated with slow decline of metabolic rates at low temperature. *Comparative Biochemistry and Physiology Part A: Molecular & Integrative Physiology, 255*, https://doi.org/10.1016/j.cbpa.2021.110920

Toxopeus, J., Dowle, E. J., Andaloori, L., & Ragland, G. J. (2024). Variation in thermal sensitivity of diapause development among individuals and over time predicts life history timing in a univoltine insect. *The American Naturalist, 203*(6), E200-E217. https://doi.org/10.1086/729515

van der Burg, K. R. L., Gauthier, J., Roe, A. D., Cusson, M., Boyle, B., Levesque, R. C., & Marshall, K. E. (2024). *Major changes in gene expression between strains of diapausing and non-diapause spruce budworm despite little evidence of genetic divergence.* bioRχiv. https://doi.org/10.1101/2024.11.20.624545

Van der Horst, D. J., & Ryan, R. O. (2012). *Insect molecular biology and biochemistry.* Academic Press. https://doi.org/10.1016/B978-0-12-384747-8.10009-1 von Schmalensee, L., Süess, P., Roberts, K. T., Gotthard, K., & Lehmann, P. (2024). A quantitative model of temperature-dependent diapause progression. *PNAS*, *121*(36). https://doi.org/10.1073/pnas.2407057121

Wadsworth, C. B., & Dopman, E. B. (2015). Transcriptome profiling reveals mechanisms for the evolution of insect seasonality. *Journal of Experimental Biology*, *218*(22), 3611-3622. https://doi.org/10.1242/jeb.126136

Wang, X., Liu, L., Guo, S., Liu, B., Zhai, Y., Yan, S., Shen, J., Ullah, F., & Li, Z. (2023). *Tweedle* gene family of *Drosophila suzukii* (Matsumura) larva enhances the basal tolerance to cold and hypoxia. *Pest Management Science*, *79*(9), 3012-3021. https://doi.org/10.1002/ps.7476

Wickham, H. (2016). ggplot2: Elegant graphics for data analysis. R package version 3.5.2. https://ggplot2.tidyverse.org

Wilsterman, K., Ballinger, M. A., & Williams, C. M. (2021). A unifying, eco-physiological framework for animal dormancy. *Functional Ecology, 35*, 11-31. https://doi.org/10.1111/1365-2435.13718

Xue, F.-S., Kallenborn, H. G., & Wei, H.-Y. (1997). Summer and winter diapause in pupae of the cabbage butterfly, Pieris melete Ménétriés. Journal of Insect Physiology, 43(8), 701-707. https://doi.org/10.1016/S0022-1910(97)00053-X

Yang, Y., & Edery, I. (2019). *Daywake*, an anti-siesta gene linked to a splicing-based thermostat from an adjoining clock gene. *Current Biology*, *29*(10), 1728-1734. https://doi.org/10.1016/j.cub.2019.04.039

Yocum, G. D., Rinehart, J. P., Horvath, D. P., Kemp, W. P., Bosch, J., Alroobi, R., & Salem, S. (2015). Key molecular processes of the diapause to post-diapause quiescence transition in the alfalfa leafcutting bee *Megachile rotundata* identified by comparative transcriptome analysis. *Physiological Entomology, 40*(2), 103-112. https://doi.org/10.1111/phen.12093

Zhang, Q., Lu, Y.-X., & Xu, W.-H. (2013). Proteomic and metabolomic profiles of larval hemolymph associated with diapause in the cotton bollworm, *Helicoverpa armigera*. *BMC Genomics, 14*(751). https://doi.org/10.1186/1471-2164-14-751